USING SIMPLE MODELS TO CHARACTERIZE LONG-TERM TRENDS AND VARIABILITY IN REGIONAL HYDROLOGY

A Dissertation

Presented to the Faculty of the Graduate School

of Cornell University

In Partial Fulfillment of the Requirements for the Degree of

Doctor of Philosophy

by

Asha Narayan Sharma

August 2014

USING SIMPLE MODELS TO CHARACTERIZE LONG-TERM TRENDS AND VARIABILITY IN REGIONAL HYDROLOGY

Asha Narayan Sharma, Ph. D.

Cornell University 2014

The three studies presented here demonstrate the utility of simple models in identifying long-term trends and variability in regional hydrology. In the first study, three new methods were used to identify the start and end of the rainy season in India. By applying these methods for data from 1951 to 2007, it was found that over much of India, the rainy season appears to have been shifting earlier. In the second study, Gravity Recovery and Climate Experiment (GRACE) satellite data were used to parameterize a simple water balance model. The model showed that evapotranspiration and storage in the Missouri River Basin have increased between 1928 and 2012. The results are consistent with the hypothesis of increasing temperatures causing the acceleration of the hydrological cycle. The third study shows that persistence patterns in precipitation, temperature, potential evapotranspiration and a drought index can be modeled using autoregressive processes where the sum of the coefficients equals 1. The results show that particular degrees of persistence are not dependent on any particular pattern of autoregression. These methods are particularly well suited to characterizing long term hydrological trends in places where there are only basic weather and streamflow data.

BIOGRAPHICAL SKETCH

Asha Narayan Sharma spent most of her childhood in Kolkata, India, where she attended Loreto House and La Martiniere for Girls. She graduated with a Bachelor of Technology degree in Industrial Biotechnology from Anna University, Chennai, India, in 2006. In 2007, she joined Cornell University to pursue a Masters of Science in Biological and Environmental Engineering, which she earned in January 2010. She has since been doing doctoral research in the same field.

To my parents and Albin.

I have much to thank you for, not least putting up with long distances and the consequences of my procrastination.

ACKNOWLEDGMENTS

Although the PhD is awarded as a recognition of individual academic achievement, there are usually many helping hands along the way. I have had the good fortune to be helped selflessly by many people over the last few years. My doctoral committee, Drs. M. Todd Walter, Michael F. Walter and Calum G. Turvey, have been a source of support, patience and guidance – thank you Todd, Mike and Cal. Several others were also generous with suggestions that helped greatly improve the quality of this research and brought to light paths for further exploration: Drs. Patrick Sullivan, Daniel Fuka, Giles Hooker, Steve Lyon and Helen Dahlke. I thank the National Center for Atmospheric Research and the Computational and Information Systems Laboratory, whose computational facilities and technical support were critical to this research. The Soil and Water Lab has been a source of camaraderie, fun, and friendships that will last a lifetime. I am so very lucky to have found myself amongst such a wonderful group of people. Over the last few years, I have had wonderful and diverse opportunities to learn from groups both on the campus and outside. Among these I would particularly like to thank the Department of Biological and Environmental Engineering, Food Systems and Poverty Reduction IGERT program, and the Tata Cornell Initiative in Agriculture and Nutrition (which also provided funding for part of this research). I am grateful to every person involved in keeping these running from day to day.

TABLE OF CONTENTS

LIST OF FIGURES

LIST OF TABLES

PREFACE

Much of the impact of long-term changes in climate will be experienced through consequent changes in hydrology. Yet it remains difficult to identify trends in the hydrological cycle due to the lack of adequate measurements, the difficulty of scaling up point measurements to larger scales and the inherent natural variability of the system. While any quantitative study requires the use of a model of some kind in order to represent the relationship between variables, these challenges in hydrology along with the desire to understand processes at a higher level of detail have led to the development of ever more complex models. These complex models can be very useful in understanding the functioning of the hydrological system, however they can be vulnerable to the very challenges they were supposed to address. For example, data limitations due to inadequate coverage of observations may be important when there is a need to apply a consistent set of assumptions across large regions. Simpler models tend to be more transparent in their assumptions and because of their generality can be more easily adapted to particular locations and scales. This can also make them more useful particularly to developing countries which often have data constraints but great needs to understand and adapt to a changing climate.

The three studies conducted as part of this dissertation build on the philosophy of using parsimonious models to understand long-term trends and variability in the hydrological cycle at a regional scale. The first study is focused on India, which gets the majority of its rainfall during three or four months in the year. There are concerns that long-term changes may be occurring in seasonality of the rainfall which is critical

to agriculture in the region. In this study, we showed that simple mathematical models such as those used in modeling bacterial growth can be used to describe the intra-annual distribution of rainfall in India. These models were applied to a gridded rainfall dataset that covers the period 1951-2007. Trends in seasonality were then identified on the basis of trends in the parameters that define the particular shape of the models. While there are significant trends in the seasonality, these tend to be of different magnitudes and even signs in different parts of India. Moreover, they occur amidst a background of a higher degree of year to year variability than popular perception leads us to believe.

The second study deals with the question of whether long-term changes in storage and evapotranspiration have occurred in the Missouri River Basin. This question is a specific case of the broader question of whether the hydrological cycle is accelerating, as is expected with rising temperatures. The challenge in answering the question is that storage and evapotranspiration are both notoriously difficult to estimate at regional scales, and few long-term records exist even for point measurements. Thus there are two "unknowns" in the water balance equation, assuming that there are reliable estimates of the other two quantities, precipitation and discharge. We addressed this by using very simple water balance model and relatively new remote sensing data. The model's one parameter describes how close actual evapotranspiration is to the potential given the storage. The model was allowed to run with a range of this parameter as well as a range of initial values of storage, generating a large number of "possible" time series of storage. The time series that best matched the satellite based estimates of recent changes in storage were selected as being the

most likely to be accurate. These show that both storage and evapotranspiration have increased in the Missouri River Basin between 1928 and 2012, consistent with the expectation of an accelerating hydrological cycle.

The third study of the dissertation relates to the issue of persistence in climatological series, here the scaled departures from expected values of precipitation, temperature, potential evapotranspiration and a drought index. Although a number of studies have been done on this topic in the last few decades, there has been a gap in terms of a clear intuitive explanation for what persistence means. We showed how different values of a commonly used estimate of persistence, the Hurst exponent, relate to the shape of a time series. Building on a recent previous study (in which I was not involved) conducted on synthetic as well as real commodity price data, we showed that persistence in the climatological variables can be modeled with these relatively simple autoregressive models. The results also showed that the order of the autoregressive model has little to do with the degree of persistence, i.e. it is possible obtain different values of the Hurst exponent with similar order. The study also showed that although there may be trends in the mean of the climatological time series, there is no evidence for an increase in variability over the last century in the region of North America that was studied.

CHAPTER 1

Is the Indian rainy season shifting in a changing climate?[1]

Chapter Summary

There are concerns that global climate change is altering the rainy season in South Asia and other places with monsoonal climates. However, it is difficult to objectively identify the start and end dates of the rainy season. This study used three methods based on daily precipitation to investigate whether the start and end dates of the rainy season in India have been systematically shifting since 1951. We also compared these results to those based on a previously published method that uses sequential 5-day rainfall totals (pentads) to identify the start and end of the rainy season. Although the methods based on daily rainfall determined different start and end dates, they all show that over most of India, the start of the rainy season has been shifting earlier over the past six decades, although there is considerable inter-annual variability. The pentad-based method showed similar changes in the rainy season, albeit for a notably smaller portion of India. Changes in the rainy season lengths are less obvious and appear to be localized. This analysis is a precursor to identifying changes in rainfall characteristics within the rainy season and impacts of shifts in the rainy season on agriculture.

[1] Asha N. Sharma, Patrick J. Sullivan, Daniel R. Fuka, Calum G. Turvey, Michael F. Walter, M.Todd Walter. Is the Indian rainy season shifting in a changing climate? <Internal review>

Introduction

South Asia is among the most densely populated regions of the world. Agriculture is regionally important as a means of income and food security and, therefore, changes in precipitation in this region could influence the well-being of a large part of the world's population. Many studies have found that the precipitation patterns in the whole region as well as its various sub-regions have been changing over the past several decades [e.g. *Dash et al.*, 2009; *Guhathakurta et al.*, 2011; *Singh and Ranade*, 2010]. Of these studies, many focus on India, perhaps because of the origin of the researchers as well as the potential availability of long-term data. Much of the rain in India and the rest of South Asia falls during the summer monsoons, which occur approximately from June to September, and this period has been the focus of many studies. For example, Dash et al. [2009] found that frequencies of moderate and low rain days in the June-September period have decreased in the 1951-2004 period over much of India. The same study found a tendency toward shorter rain spells and an increase in the number of dry spells over the same period. However, Singh and Ranade [2010] found no trends in in annual wet and dry spells over the 1951-2007 period for the same study region. Guhathakurta et al. [2011] reported a decrease in "rain days" across most of India for the period 1901-2005. Goswami et al. [2006] found no change in the total June-September rainfall in central India for 1951-2000 but an increase in the frequency of extreme events compensated by a decrease in the frequency of moderate events.

The studies mentioned above use a temporal resolution of a month. However, determining the "onset" or start of the rainy season requires a finer temporal resolution. The India Meteorological Department (IMD) defines monsoon onset over Kerala state on the basis of three indicators: (1)

precipitation after May 10th exceeds 2.5 mm on two consecutive days in 8 out of 14 specific stations, (2) outgoing longwave radiation is below 200 W m^{-2}, and (3) certain wind field conditions are met This definition has been used by some studies [e.g. *Raju et al.*, 2007; *Joseph*, 2004; *Chandrasekar*, 2010]. While this method of identifying the onset of the monsoon is useful in identifying changes in the monsoon as a meteorological phenomenon, focusing primarily on precipitation is more relevant to how monsoonal changes could impact hydrology and agriculture.

A variety of other definitions for monsoon onset are based on a precipitation threshold at some proportion of a specific set of Indian Meteorological Department (IMD) stations (Normal Dates for Onset of Southwest Monsoon, available from India Meteorological Department, http://www.imd.gov.in/). Using an IMD dataset of monsoon onset dates based on one of these methods, Goswami et al. [2010] found that the onset difference between Trivandrum and Nagpur, India has increased between 1960 and 2007. This indicates that the progression of the monsoon, i.e. the pace at which monsoonal rainfall moves from the coast inland, has slowed over this time period. They conclude that this slowdown is caused by a weakening of vertical easterly shear of zonal winds and gradient of specific humidity in the 60-90 °E and 10°S-equator region Goswami et al. [2010]. While the method used to identify monsoon onset in their study was based only on precipitation, reliance on data from specific stations makes the definition very specific to the neighborhood of those stations.

Wang and LinHo [2002] provided a much-used definition of monsoon based only on precipitation records at a given place or grid cell (i.e., based on gridded reanalysis data). Their method used pentads, i.e. non-overlapping sequences of five-day-average precipitation. They

defined the onset of the monsoon across Asia as the first pentad in the May-September period in which the mean daily precipitation exceeded the January mean by at least 5 mm. Kajikawa et al. [2012] analyzed differences in monsoon onset across a large part of Asia between 1979-1993 and 1994-2008 using this method and found that monsoon onset by this definition came 2 to 6 pentads earlier over northwest India in the latter period and 2 to 8 pentads later in parts of peninsular India, and Myanmar; Northeast India did not have a consistent regional shift in the monsoon onset. Ashfaq et al. [2009] used the RegCM3 nested climate model to predict the response of the Asian summer monsoon to greenhouse gas forcing in 2071-2100 using the IPCC A2 scenario and found that the onset of the monsoon would be 2 to 4 pentads later across much of South Asia by the end of this century compared to the 1961-1990 onsets determined by Wang and LinHo [2002].

While the method of Wang and LinHo [2002] depends only on the precipitation record, by virtue of averaging over five day periods, it may be missing trends that have been smaller, but which might still be substantial from an agricultural standpoint in the long run. With all the methods described above, the use of thresholds and the requirement in some of the methods that the threshold be exceeded at a certain proportion of stations also introduces a degree of arbitrariness. Cook and Buckley [2009] suggested a procedure that addresses much of the arbitrariness by fitting two intersecting straight lines to each of two separate windows in the annual cumulative precipitation time series. The point of intersection in the early and late windows denoted the start and end of the rainy season, respectively. This method relies on the specification of the windows, which may vary substantially over a large geographic area. The objectives of this study are to first introduce three new methods to identify the start and end of the rainy season based on the daily precipitation record, compare them to each other and to the pentad method of Wang and

LinHo [2002], and then to examine the trends in the rainy season using these different methods. The new methods do not rely on arbitrary thresholds of precipitation, and are therefore applicable to any location that experiences a single or primary rainy season. They may also be adapted for multimodal rainy seasons, though this aspect is outside the scope of this study.

Methods

In this study, we use the IMD's 1-degree gridded daily dataset for India for the period 1951-2007. The R software [*R Core Team*, 2012] was used to perform the analyses using the National Center for Atmospheric Research's computing resources [*Computational and Information Systems Laboratory*, 2012]. The start of the rainy season was calculated in three new ways.

The first involved fitting a smoothed spline (SS) to the cumulative precipitation data, normalized by the annual total precipitation. We used the R package, grofit [*Kahm et al.*, 2010], to do this. The start of the rainy season is defined by the point where the tangent of the point of maximal slope intersects the x-axis (Fig. 1.1a). The end of the rainy season is calculated similarly, with the cumulative precipitation calculated in reverse, i.e. from the end of the year to the beginning. This method was originally intended to fit biological growth models, but the general nature of the method makes it appropriate for use in this situation. The point where the tangent of the point of maximal slope intersects the x-axis is referred to as the lag-time in biological growth models [*Zwietering et al.*, 1990], and is a measure of the time before the growth (or in this case cumulative precipitation) increases at a much greater rate.

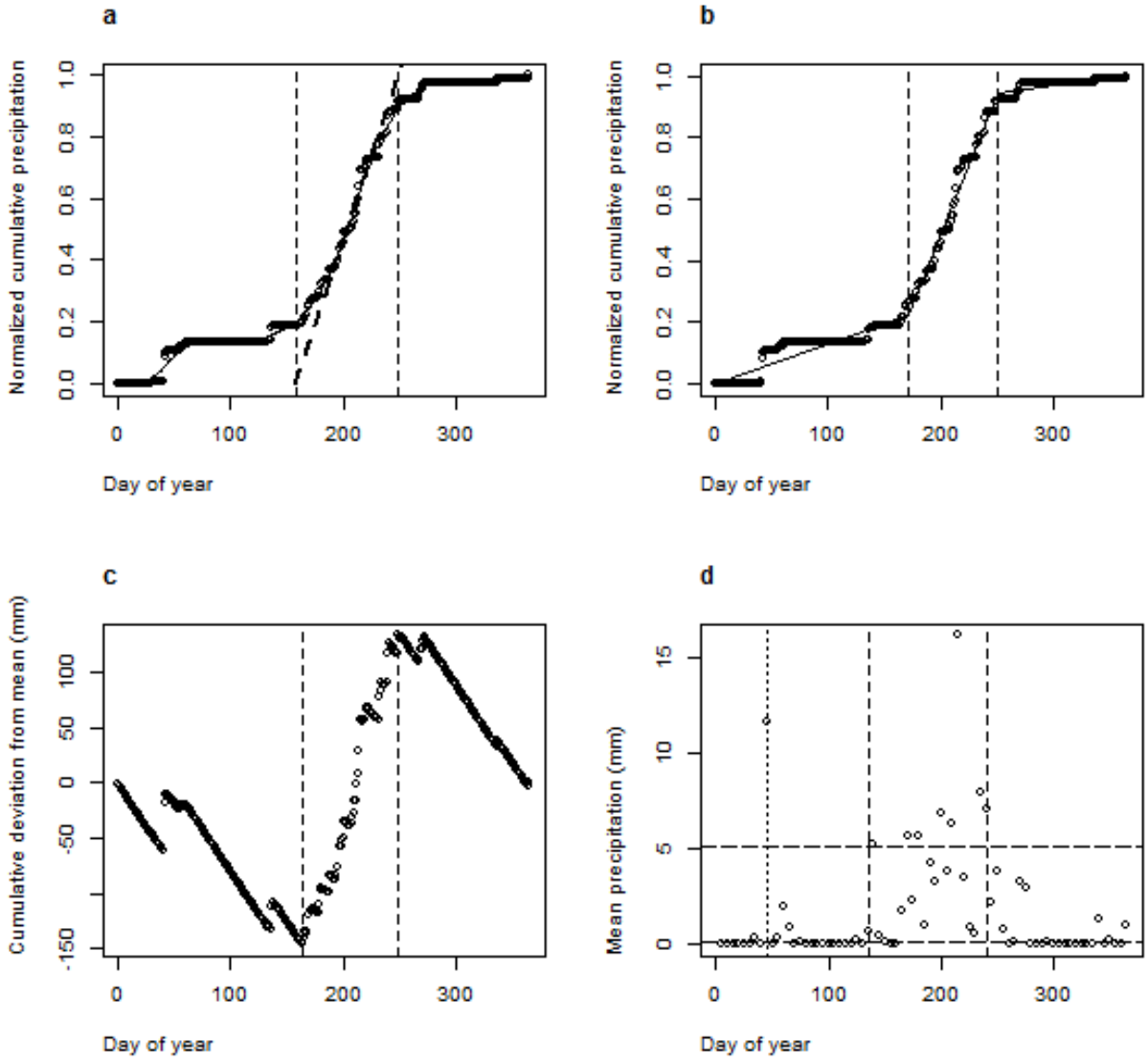

Figure 1.1: Example of methods used to define start and end of the rainy season (vertical dashed lines) for the grid cell corresponding to 79.5 °E, 20.5 °N: (a) SS, (b) PL, (c) CD, and (d) WL methods. In (d), the lower horizontal dashed line corresponds to the January mean precipitation, the upper horizontal dashed line corresponds to the threshold indicating the start of the monsoon (January mean precipitation plus 5 mm); the vertical dotted line near day 40 shows the first pentad where the threshold is exceeded to illustrate why the WL method includes the caveat that the rainy season be constrained to the May-September period.

A second method to define the start and end of the rainy season involved fitting a piecewise linear model (PL) with two breakpoints to the cumulative annual precipitation (Fig. 1.1b). In PL, the data are fit by three straight lines, each with a different slope and intercept, with the first two lines intersect at the first breakpoint and the last two lines at the second breakpoint. Since in general the middle line has the steepest slope due to the high rate of increase of cumulative precipitation in the middle of the year, the two breakpoints are taken to be representative of the start and end of the rainy season. The R package, segmented [*Muggeo*, 2008], was used to estimate these points.

The third method (denoted "CD") derives from the method introduced by Cayan et al. [2001] to study snowmelt in US rivers. The cumulative departure (D_n) from the mean precipitation $\bar{p}$ for the year is calculated (Fig. 1.1c):

$$D_n = \sum_{i=1}^{n}(p_i - \bar{p}) \quad (1)$$

where p_i represents the precipitation on day i. The minimum and the maximum of the D_n series are taken to represent the start and end, respectively, of the rainy season. These three methods represent three objective but distinct approaches to defining the start and end of the rainy season.

The method of Wang and LinHo [2002] (WL) is used for comparison (Fig. 1.1d). The start and end of the rainy season are defined as the first and last pentads, respectively, to exceed the 5 mm day^{-1} threshold in this time period. To focus on locations where these methods are most reliable, we excluded grid cells where the standard deviation of the start of the rainy season exceeded 30 days in any of the three (SS, PL, CD) methods introduced here (Fig. A1.2).

In order to improve the robustness of the analysis, we used the maximum entropy bootstrap (MEB) [*Vinod*, 2004], available through the R meboot package [*Vinod*, 2009], to generate 1000 alternative time series for each of the selected grid cells for each year. For each year and grid cell combination, therefore, we obtained 1000 values of the start and end of the rainy season by each method (SS, PL, CD and WL). The median of these 1000 values were taken as being representative for the year-grid cell combination. The MEB algorithm satisfies the ergodic and central limit theorems, and is different from "traditional" bootstrapping which tend to lose time dependence information (i.e. x_t follows x_{t-1} which follows x_{t-2}) [*Vinod*, 2004]. Since the MEB does not require the time series to be stationary, it is appropriate for many climatic time series [*Barbosa*, 2011; *Cook and Buckley*, 2009]

Results

The four methods (SS, PL, CD, and WL) agree surprisingly well on the broad spatial patterns of start of the rainy season (Fig. 1.2), e.g. the early start in the east and the late start in the northwest. Although the methods are somewhat less consistent in generating the spatial patterns for the end of the rainy season, the all generally show an earlier end in the west than in the east (Fig. 1.3); variability across methods is relatively high but comparable (Fig. A1.1).

The WL method is much less variable in terms of the end of the rainy season, however this is not surprising since that method uses five day precipitation averages and that the rainy season start and end pentads are constrained to be in the May-September period. The WL method is somewhat unique in that produces fairly constant rainy season start-dates for the early start-dates, i.e., where the other three methods estimate start-dates earlier than day 140 (Fig. 1.4a-c), which

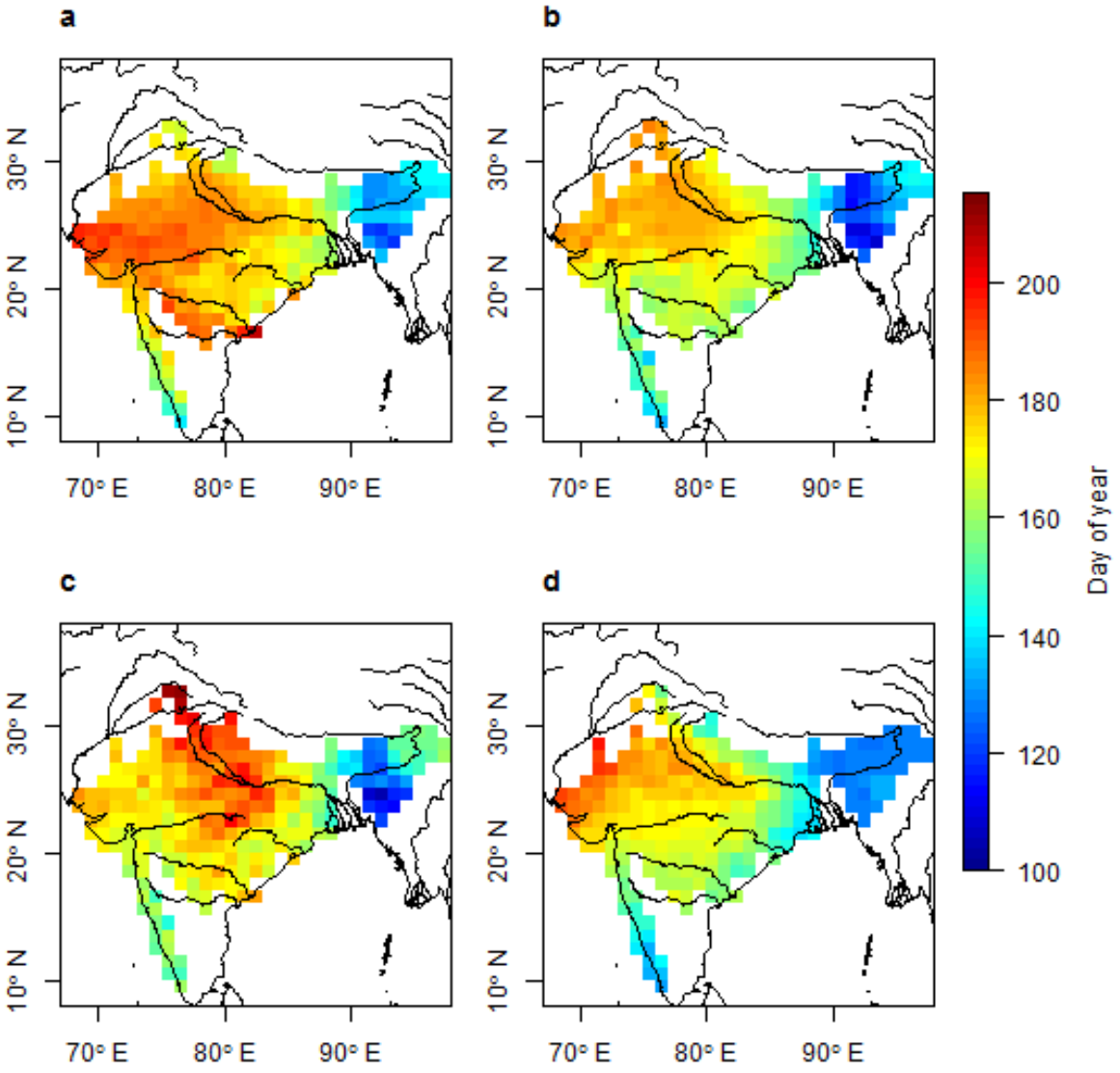

Figure 1.2: Mean start of the rainy season for the period 1951-2007 determined by the (a) SS, (b) PL , (c) CD and (d) WL methods. Only grid cells which have a standard deviation of 30 days or less in the start of the rainy season by the SS, PL and CD methods are included in this analysis.

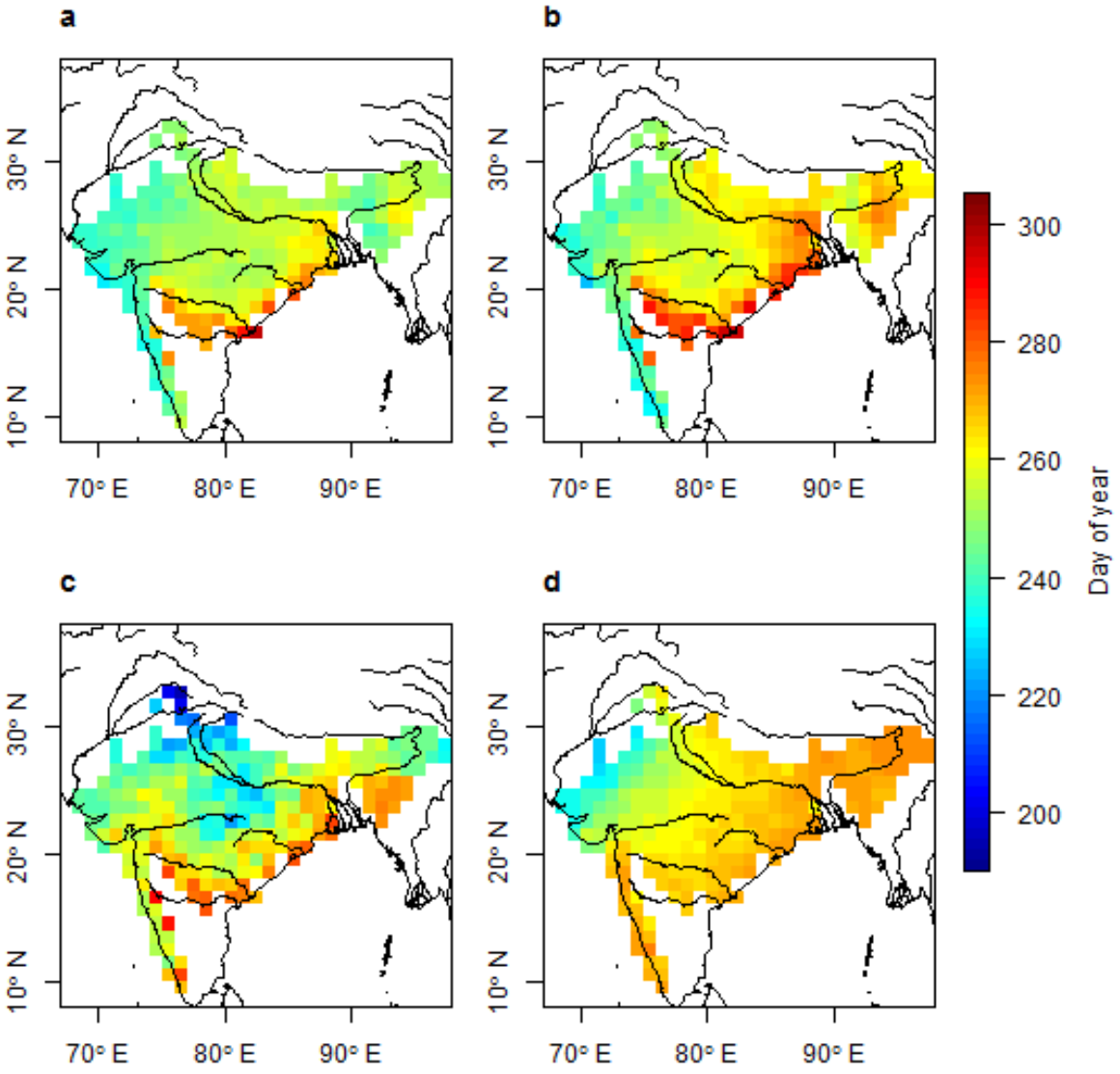

Figure 1.3: Mean *end* of the rainy season for the period 1951-2007 determined by the (a) SS, (b) PL, (c) CD and (d) WL methods.

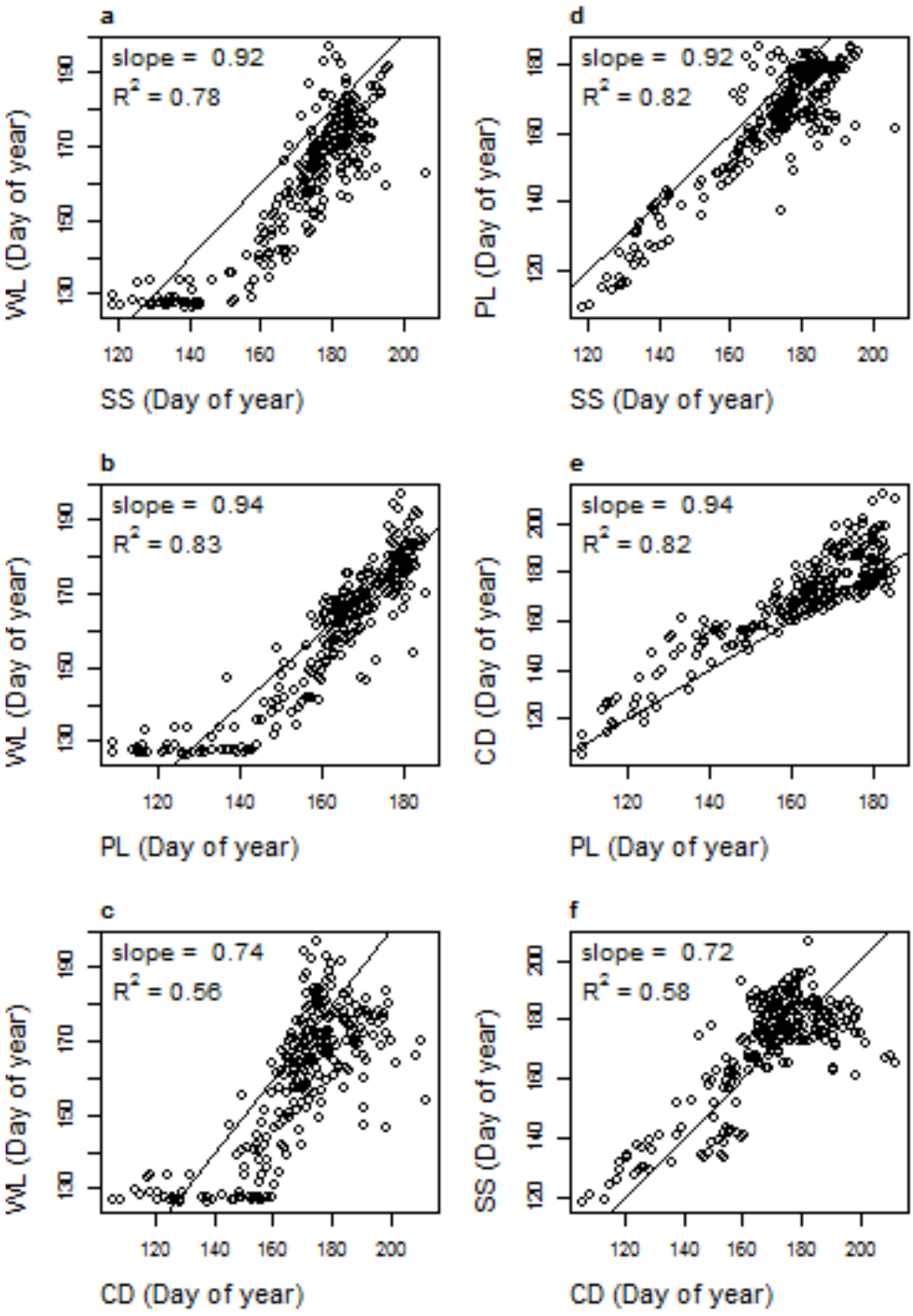

Figure 1.4: Mean (1951-2007) start date of the rainy season for each grid cell in the selected region calculated by the various methods plotted against each other. The 1:1 line is also shown.

is likely an artifact of constraining the rainy season to May-September. In general, the SS method shows the latest start to the rainy season and the CD method shows the earliest. All three new methods are linearly related to each other and are close to the 1:1 line (Fig. 1.4d-f). The difference between the WL method and the others is more pronounced for the end of the rainy season (Fig. 1.5a-c). In general, the methods vary more from each other for the end of the rainy season than when used to estimate the start of the rainy season. Here the SS method shows the earliest end to the rainy season whereas the CD method shows the latest end.

Despite the broad similarities across methods in terms of the *spatial* patterns of start and end of the rainy season, the differences across methods (Figs. 1.4 and 1.5) result in substantial differences in the proportion of the annual precipitation that occurs in the rainy season (Fig. 1.6). For example, the CD method, which tends to have the earliest starts and the latest ends, defines a longer rainy season (Fig. A1.4) and accounts for a larger proportion of annual precipitation (Fig. 1.6). The difference in the length of the monsoon as calculated by the CD and SS methods is generally 15-30 days and results in 10-20 % differences in the percentage of annual precipitation falling during the rainy season (Fig. A1.5).

All the methods indicate that the rainy season is starting earlier in most places, with smaller scattered locations where it is starting later, mostly concentrated in the far east of the region (Fig. 1.7). The WL method shows the least grid cells (26 % of all grid cells considered) with any significant ($p<0.05$) trend. Both the SS and PL methods show some similar patterns of later rainy season start-dates in central India, parts of southern India and northeastern India (red grid cells in Fig. 1.7a-b). The WL method similarly shows very few locations with any significant trend in the end of the rainy season (Fig. A1.6). The methods show broad consensus in identifying an earlier

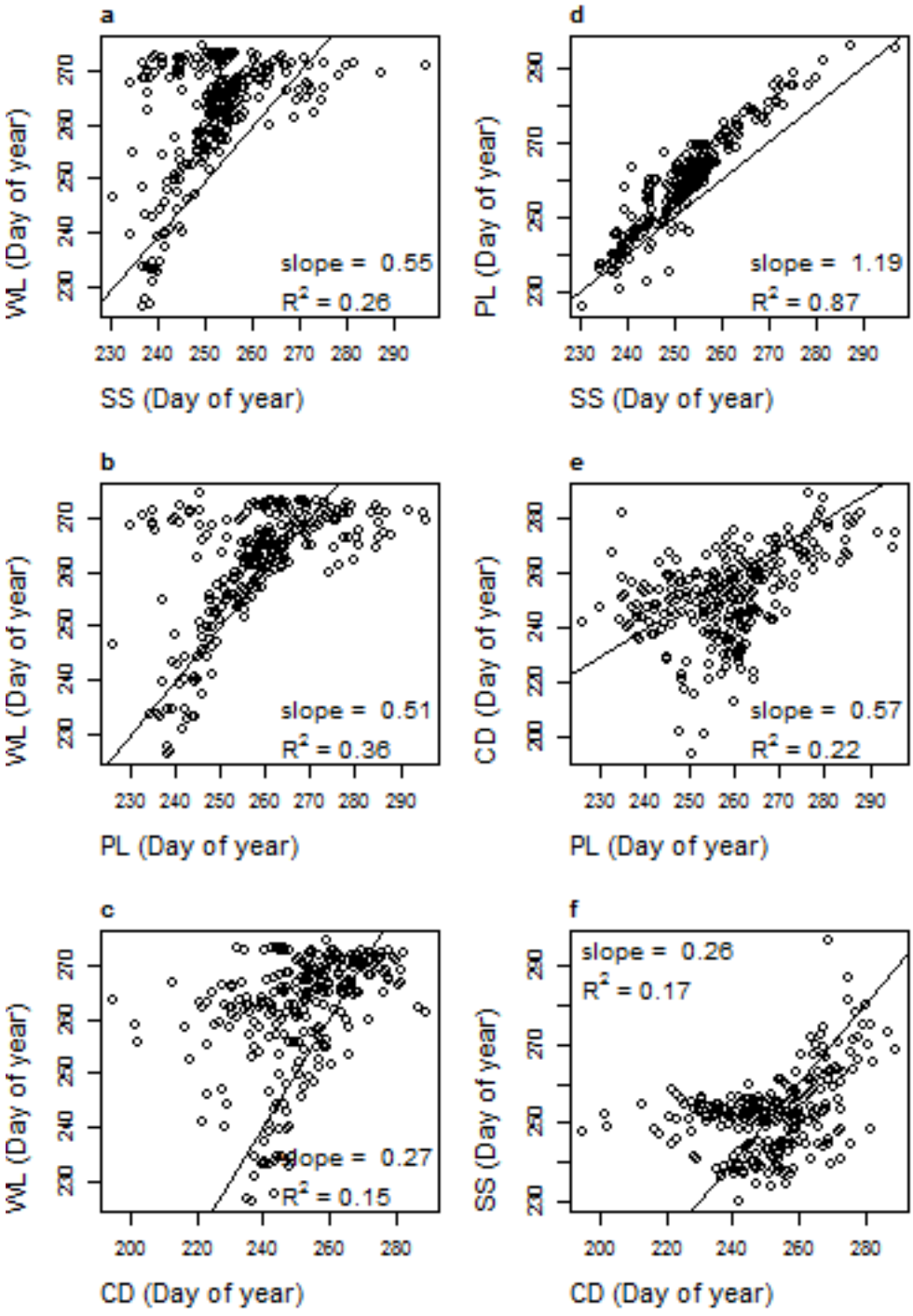

Figure 1.5: Mean (1951-2007) end date of the rainy season for each grid cell in the selected region calculated by the various methods plotted against each other. The 1:1 line is also shown.

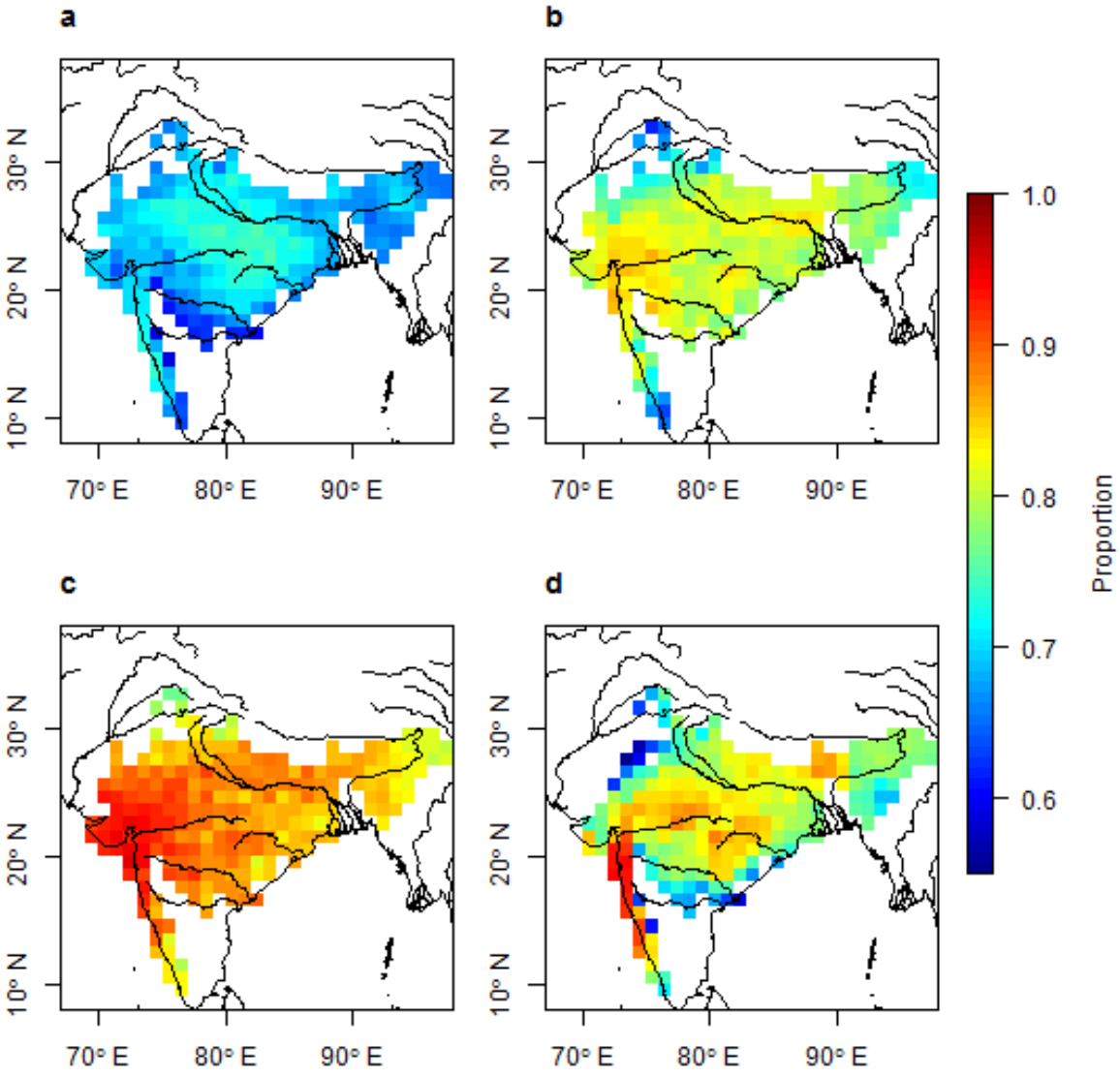

Figure 1.6: Mean proportion of total annual precipitation that falls during the rainy season for the period 1951-2007 determined by the (a) SS, (b) PL, (c) CD and (d) WL methods.

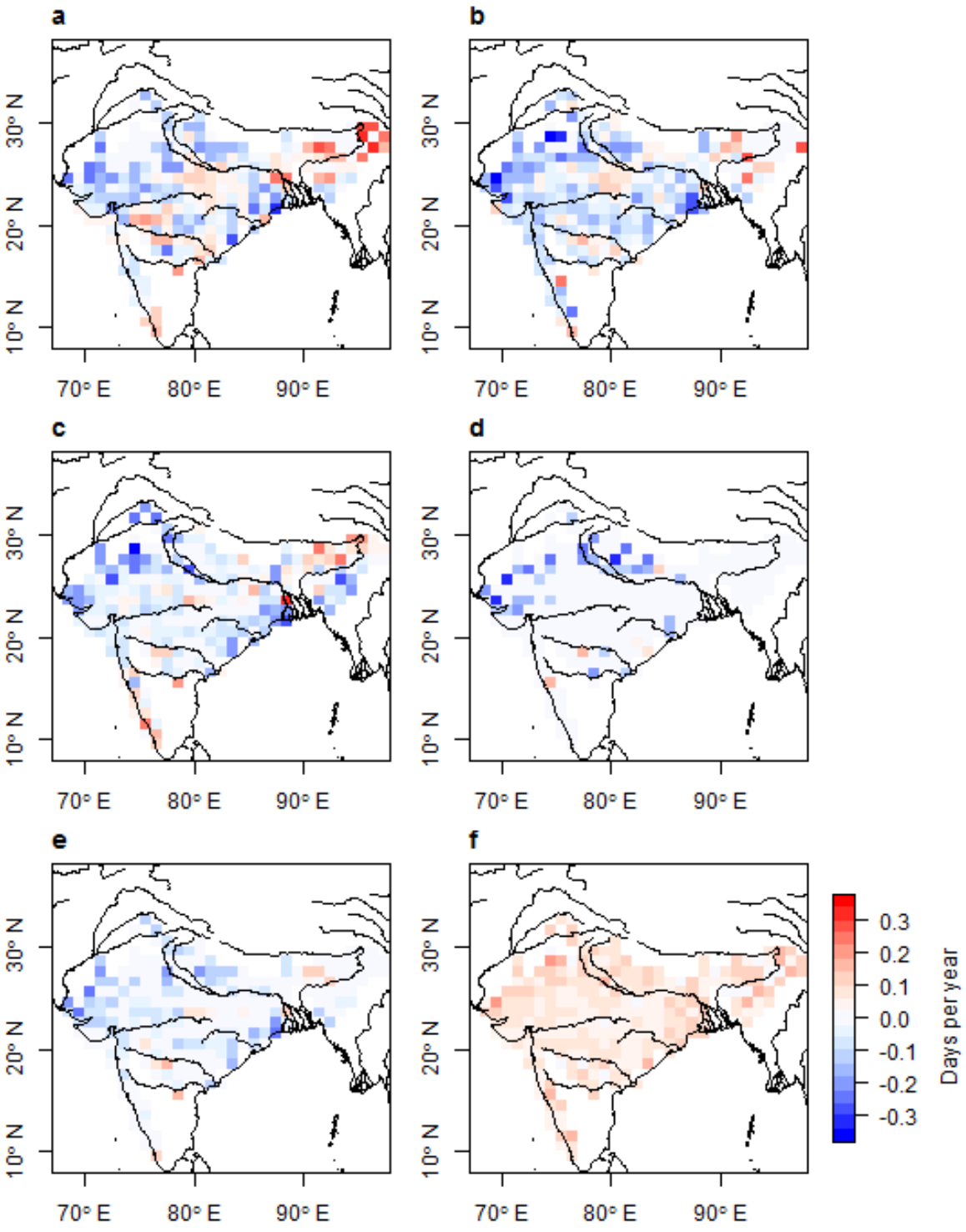

Figure 1.7: Trend in *start* of the rainy season (days per year) for the period 1951-2007 determined by the (a) SS, (b) PL, (c) CD and (d) WL methods; (e) the median trend and (f) the standard deviation of the trends. Non-zero median trends are shown only if three or more methods agreed on the direction of the trend. Only significant ($p<0.05$) trends are shown.

start to the rainy season across much of the study region except the northeastern part (Fig. 1.7e), though they vary greatly in the magnitude of the shifts identified (Fig. 1.7f).

There is considerably more spatial variation and less consensus among the methods for the regarding the trends in the length of the rainy season (Fig. 1.8). However, for most grid cells where the trends do agree, they agree on a lengthening rainy season. It is remarkable that despite their differences in the ways we estimated the start and end of the rainy season, all the methods show an increase in the length of the rainy season over the delta region in the east (around 23 °N, 88 °E) and in the north near the major rivers (around 28 °N, 80 °E). The variation across methods in the trend in the length of the rainy season, despite the greater consensus in the trend of the start, may be explained by the spatial patterns of the trends in the end of the rainy season (Fig. A1.6). The end of the rainy season shows little consensus among methods over many of the grid cells in which there is consensus on trends in the rainy season start. However, the various methods seem to agree on an earlier end in regions in the west (around 28 °N, 75 °E) and a later one over the northeast (26 °N, 90 °E).

The trends in the amount of precipitation during the rainy season show a decrease across most of central India (> 64% of grid cells in this region), regardless of method used (not shown). The exception is the eastern delta region, where there is an increase in precipitation during the rainy season regardless of method. The similarity in precipitation patterns regardless of the differences in the rainy season length can be explained by the fact that there are spatially similar patterns in annual total precipitation (Fig. A1.8), and the rainy season, defined by any of the methods, accounts for most of the annual total precipitation (Fig. 1.6).

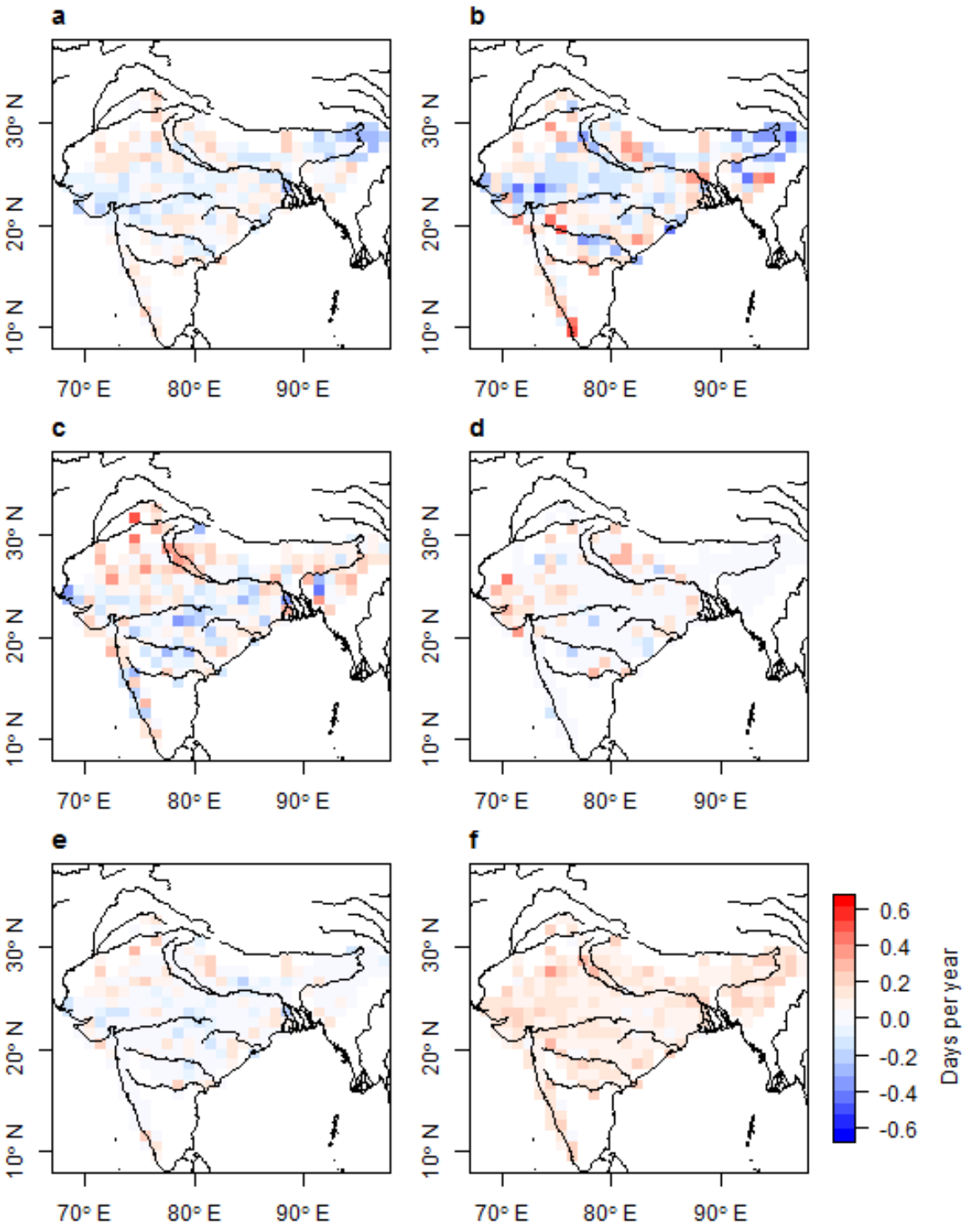

Figure 1.8: Trend in length of the rainy season for the period 1951-2007 determined by the (a) SS, (b) PL, (c) CD and (d) WL methods; (e) the median trend and (f) the standard deviation of the trends. Non-zero median trends are shown only if three or more methods agreed on the direction of the trend. Only significant ($p<0.05$) trends are shown.

Discussion

The methods presented here represent three approaches to objectively identify the start and end of the rainy season in monsoonal climates. These represent an attempt not to replace the meteorological definitions of the phenomena that cause the distinct rainy season, but rather an attempt to characterize the intra-annual distribution of precipitation. The approaches used here derive from attempts to identify change-points in time series of other variables (such as bacterial growth and discharge in streams fed by snowmelt) but are new to this application. They are all appealing in their lack of dependency on arbitrary thresholds to identify the change-points in precipitation in monsoonal climates. The monsoonal rains are critical to food and income security in South Asia. There is therefore good reason to explore alternative ways of identifying long-term changes in rainfall seasonality in this region. The relative utility of these methods may be estimated by their ability to explain variations in relevant outcomes, such as crop yields; however, that is beyond the scope of this study.

We show here that regardless of method chosen, the rainy season in much of India has been starting earlier over the past few decades. This has been suggested by earlier studies that used monthly and pentad measures [e.g.*Kajikawa et al.*, 2012]. However, these previously published measures may be missing some of the trends that can be captured by the methods proposed here that use daily data. For example, the WL method, which is based on pentads, does not show the trends in the start of the rainy season in some regions which are detected by the three other methods (Fig. 1.7). The In particular, WL method does not capture the trend towards a delayed start of the rainy season in northeastern India.

The causes for changes in the behavior of precipitation in India and, more generally, South Asia, are the subject of much current research. The Asian monsoons, of which the Indian summer monsoon is part, are characterized by annual reversals of prevailing winds, which are controlled by the thermal contrast between land and ocean [*Wang and LinHo*, 2002]. Several hypotheses exist regarding the drivers of the monsoon. A widely accepted hypothesis is that in the pre-monsoon season, the heating over the Tibetan Plateau causes the rise of warm air over this region, which in turn causes moisture laden air from the ocean to flow in [*Gautam et al.*, 2009]. However, alternative hypotheses have also been proposed, such as the "insulation effect" of the Himalayas of warm moist air over India from the cooler and drier air north of the Himalayas [*Boos*, 2010]. Kajikawa et al. [2012] suggest that the cause for the trend towards an earlier onset of the monsoon in much of Asia, as detected from monthly and pentad data, is due to the heating over the landmass in Asia, particularly over the 30° N region, in May, which led to an increased thermal contrast between land and ocean earlier in the year. A previous study over the same time period (1979-2007) found that the warming of the troposphere over the Himalayan-Gangetic region led to a greater land-ocean temperature gradient, particular to the pre-monsoon period [*Gautam et al.*, 2009]. Other explanations may also be possible: for example, agricultural intensification in northern India in April, as represented by normalized difference vegetation index NDVI in that month, correlates with a decreased July precipitation in peninsular India over the period 1951-2003, possibly due to net radiative cooling or changes in mesoscale convection [*Niyogi et al.*, 2010].

Kitoh et al. [2013] found that projections by 29 climate models under a variety of scenarios indicate an earlier onset and later retreat of the monsoon for the period 2080-2099 versus the reference period of 1986-2005 in many parts of the Asian summer monsoon region, though the

reason for these changes is unclear. They note there is a high degree of agreement between models in South Asia, which in their study excludes western India and Pakistan, and includes regions in Tibet and southern China. The trend towards later ending in our study is prominent in northeastern India, which is on the edge in our study, but quite central to the South Asian region as defined by Kitoh et al. [2013]. However, we find that the rainy season in northeastern India also shows a trend towards a later start, seemingly in contrast to the results of Kitoh et al. [2013] for the longer-term. This could be explained by the small trend found by them for the region – which could be because of a reversal in the long term of the trend we find, the aggregation of opposite trends in different parts of the region, or because of characteristics of the models they used.

While many of the other studies that focus on the rainy season in South Asia define it as the monsoon, we make no similar claim here. The methods described here need not correspond exactly with the meteorological phenomenon of the monsoon – indeed the end dates according to the SS and PL methods are much earlier than the monsoon end dates as determined by the IMD (Normal Dates for Onset of Southwest Monsoon, available from India Meteorological Department, http://www.imd.gov.in/), which are determined by a combination of precipitation, wind field and outgoing longwave radiation measures. Rather, our intention here is to estimate in an objective way and purely on the basis of the precipitation some key measures of the seasonality of precipitation, and then to use these to better understand the trends and variability of this seasonality. While the WL method has been popular, possibly for its simplicity, it has some arbitrary (or at least poorly justified) assumptions such as the use of the January mean, 5 mm day^{-1} rainfall threshold, the use of pentads, and the need to constrain the period considered from May to September to avoid spurious start dates (Fig. 1.1d). While these seemingly arbitrary

assumptions may be reasonable in much of monsoonal Asia, having objective methods like those presented here will not require stationarity in the thresholds and may inspire more confidence in the reliability of the results of an analysis.

This study shows that the start and end of the rainy season as determined by precipitation-only measures vary greatly year-to-year at the 1°-grid scale used here. This is true even when using the method of Wang and LinHo [2002], which has been widely used in the literature on this subject (Fig. A1.1). The inter-annual variability in the monsoons was noted as early as 1967 by Ananthakrishnan et al. [1967]) who made the observation that "There is a general impression that the southwest monsoon is a meteorological phenomenon of the Asian tropics that repeats year after year with great regularity and in a nearly identical manner. The factual position, however, is that large variations occur from year to year not only in the date and manner of its initial onset, but also in the spatial and temporal distribution of rainfall over the country." The high variability makes it difficult both to arrive at an objective definition of the start and end of the rainy season as well as to detect a trend using such a definition. For this study, we used an ensemble of three methods (SS, PL and CD) that have previously not been used in the context of determining seasonality of precipitation. The comparison in rainy season start and end dates between methods shows that they detect different stages of the annual cycle of precipitation. The three methods introduced here are more sensitive to detecting long-term trends than the WL method (Fig. 1.4 and 1.5).

Given the strong correlation between the start dates predicted by the various methods, especially the SS, PL, and CD, it might be expected that the trends shown by the different methods would be strongly correlated. However the methods are poorly correlated in terms of absolute trends,

although they do generally agree with respect to the direction of the trends (Fig. A1.7). This indicates that the relationship between the different methods can be highly variable for a given grid cell from year to year, even though they maintain a consistent relationship for the 57-year averages across the whole study region (Fig. 1.4). Since it is not obvious that any of these new methods is more reliable than the other, it is useful to examine the range of trends demonstrated by the various methods. The early identification of such trends can be useful for agricultural and water resources planning and management. There seems to be a clear trend in the start of the rainy season in much of the study region - it is shifting earlier in most places except the northeast, where it seems to be shifting later. Rosenzweig and Binswanger [1993] found profits were negatively affected by later monsoon onset, which they defined as "the date after which there has been at least 20 mm of rain within several consecutive days after 1 June." However, it is not clear what effect, if any, the trends in the start of the rainy season seen in our study may have had on crop productivity and profits. Such an effect would likely be difficult to detect due to the effects of precipitation amount, spells of wet and dry weather, temperatures, crop inputs and crop types in addition to the variability of the rainy season start date; linking changes in rainfall patterns to agricultural production should be a research topic in the near future.

Unlike the rainy season start-date trends, the trends in the end-date, and consequently, the length of the rainy season are mixed. Presumably the impact of these trends would vary by crop type, soil, and crop management practices in addition to other climate variables. It is possible that the rainy season start date shows a more consistent trend because the start of the Indian summer monsoon is a much more "distinct" meteorological phenomenon than its end. The decline in precipitation amount seen in most places will likely affect crop yields negatively [e.g. 1999; *Lal et al.*, 1999], although it seems the relationship of rainfall amount to crop yields is complicated

[*Clarke et al.*, 2012]. Increasing variability can be a concern for agriculture; however we find no evidence of consistent trends in variability of the rainy season start and end over the study period as calculated by trends in standard deviation of moving 11 year windows (data not shown).

Conclusions

The dates of the rainy season as well as the amount of precipitation are important characteristics for agriculture throughout the world, but especially in primarily rain-fed systems. Here we introduce some new, objective methods to "define" the start and end of the rainy season at a daily resolution, in order to identify trends and variability in the rainy season in India. We find that the start and end of the rainy season tend to be highly variable from year to year in many parts of India, and that the start of the rainy season is shifting – with a trend towards an earlier start in most of India although it is starting later primarily in the Northeast. The end and length of the rainy season show strong, but mixed, trends with seemingly less agreement between models. The methods presented here can be adapted to other regions with unimodal distinct rainy seasons. We believe the general methodological approaches shown here could be generalized to multi-modal rainy seasons as well.

References

Ananthakrishnan, R., U. R. Acharya, and A. R. Ramakrishnan (1967), On the criteria for declaring the onset of the southwest monsoon over India. Rep. IV 18.1, India Meteorol. Dep., Pune.

Ashfaq, M., Y. Shi, W.-w. Tung, R. J. Trapp, X. Gao, J. S. Pal, and N. S. Diffenbaugh (2009), Suppression of south Asian summer monsoon precipitation in the 21st century, Geophys. Res. Lett., 36, L01704, doi:10.1029/2008GL036500.

Barbosa, S. M. (2011), Testing for deterministic trends in global sea surface temperature, J. Climate, 24(10), 2516-2522, doi:10.1175/2010JCLI3877.1.

Boos, W. R. K. Z. (2010), Dominant control of the South Asian monsoon by orographic insulation versus plateau heating, Nature, 463, 218-222, doi: 10.1038/nature08707.

Cayan, D. R., M. D. Dettinger, S. A. Kammerdiener, J. M. Caprio, and D. H. Peterson (2001), Changes in the onset of spring in the western United States, Bull. Amer. Meteor. Soc., 82(3), 399-415, doi: 10.1175/1520-0477(2001)082<0399:CITOOS>2.3.CO;2.

Chandrasekar, M. V. R. Sesha Sai, P. S. Roy, and R. S. Dwevedi (2010), Land Surface Water Index (LSWI) response to rainfall and NDVI using the MODIS Vegetation Index product, Int. J. of Remote Sens., 31(15), 3987-4005, doi: 10.1080/01431160802575653.

Clarke, D. J., O. Mahul, K. Rao, N., and N. Verma (2012), Weather-based crop insurance in India, Rep. 5985, World Bank, Washington, D.C., doi: 10.1596/1813-9450-5985.

Computational and Information Systems Laboratory. 2012. Yellowstone: IBM iDataPlex System (University Community Computing). National Center for Atmospheric Research, Boulder, Colorado, http://n2t.net/ark:/85065/d7wd3xhc.

Cook, B. I., and B. M. Buckley (2009), Objective determination of monsoon season onset, withdrawal, and length, J. Geophys. Res., 114, D23109, doi:10.1029/2009JD012795.

Dash, S. K., M. A. Kulkarni, U. C. Mohanty, and K. Prasad (2009), Changes in the characteristics of rain events in India, J. Geophys. Res., 114, D10109, doi:10.1029/2008JD010572.

Gautam, R., N. C. Hsu, K.-M. Lau, S.-C. Tsay, and M. Kafatos (2009), Enhanced pre-monsoon warming over the Himalayan-Gangetic region from 1979 to 2007, Geophys. Res. Lett., 36, L07704, doi:10.1029/2009GL037641.

Goswami, B. N., J. R. Kulkarni, V. R. Mujumdar, and R. Chattopadhyay (2010), On factors responsible for recent secular trend in the onset phase of monsoon intraseasonal oscillations, Int. J. Climatol., 30(14), 2240-2246, doi: 10.1002/joc.2041

Goswami, B. N., V. Venugopal, D. Sengupta, M. S. Madhusoodanan, and P. K. Xavier (2006), Increasing trend of extreme rain events over India in a warming environment, Science, 314(5804), 1442-1445, doi: 10.1126/science.1132027.

Guhathakurta, P., O. P. Sreejith, and P. A. Menon (2011), Impact of climate change on extreme rainfall events and flood risk in India, J Earth Syst. Sci., 120(3), 359-373, doi: 10.1007/s12040-011-0082-5.

Joseph, P. V. and S. Sijikumar (2004), Intraseasonal Variability of the Low-Level Jet Stream of the Asian Summer Monsoon, J. Climate, 17(7), 1449-1458, doi: 10.1175/1520-0442(2004)017<1449:IVOTLJ>2.0.CO;2.

Kahm, M., G. Hasenbrink, H. Lichtenberg-Frate, J. Ludwig and M. Kschischo (2010), grofit: Fitting biological growth curves with R, J. Stat. Soft., 33(7), 1-21.

Kajikawa, Y., T. Yasunari, S. Yoshida, and H. Fujinami (2012), Advanced Asian summer monsoon onset in recent decades, Geophys. Res. Lett., 39, L03803, doi:10.1029/2011GL050540.

Kitoh, A., H. Endo, K. Krishna Kumar, I. F. A. Cavalcanti, P. Goswami, and T. Zhou (2013), Monsoons in a changing world: A regional perspective in a global context, J. Geophys. Res. Atmos., 118, 3053–3065, doi:10.1002/jgrd.50258.

Lal, M., K. K. Singh, G. Srinivasan, L. S. Rathore, D. Naidu, and C. N. Tripathi (1999), Growth and yield responses of soybean in Madhya Pradesh, India to climate variability and change, Agric. For. Meteorol., 93(1), 53-70, doi: 10.1016/S0168-1923(98)00105-1.

Muggeo, V. M. R. (2008), segmented: An R package to fit regression models with broken-line relationships, R News, 8(1), 20-25.

Niyogi, D., C. Kishtawal, S. Tripathi, and R. S. Govindaraju (2010), Observational evidence that agricultural intensification and land use change may be reducing the Indian summer monsoon rainfall, Water Resour. Res., 46, W03533, doi:10.1029/2008WR007082.

Raju, P., U. Mohanty, and R. Bhatla (2007), Interannual variability of onset of the summer monsoon over India and its prediction, Natural Hazards, 42(2), 287-300, doi: 10.1007/s11069-006-9089-7.

Rosenzweig, M. R., and H. P. Binswanger (1993), Wealth, weather risk and the composition and profitability of agricultural investments, Econ. J., 103(416), 56-78, doi: 10.2307/2234337.

Singh, N., and A. Ranade (2010), The wet and dry spells across India during 1951-2007, Journal of Hydrometeor., 11(1), 26-45, doi:10.1175/2009jhm1161.1.

R Core Team (2012), R: A language and environment for statistical computing. R Foundation for Statistical Computing, Vienna, Austria.

Vinod H.D. and J. Lopez-de-Lacalle (2009), Maximum entropy bootstrap for time series: The meboot R package, J. Stat. Soft., 29(5), 1-19.

Vinod, H. D. (2004), Ranking mutual funds using unconventional utility theory and stochastic dominance, J. Emp. Fin., 11(3), 353-377, doi:10.1016/j.jempfin.2003.06.002.

Wang, B., and B. LinHo (2002), Rainy Season of the Asian–Pacific Summer Monsoon, J.Climate, 15(4), 386-398, doi: 10.1175/1520-0442(2002)015<0386:RSOTAP>2.0.CO;2.

Zwietering, M., I. Jongenburger, F. Rombouts, and K. Van't Riet (1990), Modeling of the bacterial growth curve, Appl. Env. Microbiol., 56(6), 1875-1881.

CHAPTER 2

Estimating long-term changes in actual evapotranspiration and water storage using a one-parameter model[2]

Chapter Summary

Estimations of long-term regional trends in evapotranspiration (*E*) and water storage are key to our understanding of hydrology in a changing environment. Yet they are difficult to make due to the lack of long-term measurements of these quantities. Here we use a simple one-parameter model in conjunction with Gravity Recovery and Climate Experiment (GRACE) data to estimate long-term E and storage trends in the Missouri River Basin. We find that *E* has increased in the river basin over the period 1929-2012, consistent with other studies that have suggested increases in ET with a warming climate. The increase in *E* appears to be driven by an increase in precipitation and water storage because potential *E* has not changed substantially. The simplicity of the method and its minimal data requirements provide a transparent approach to assessing long-term changes in hydrological fluxes and storages and may be applicable to regions where meteorological and hydrological data are scarce.

Introduction

Terrestrial water storage is critical to many ecosystem services [*Brauman et al.*, 2007]. Moreover, it is expected that increased hydrologic variability associated with climate change is

[2] Asha N. Sharma, M. Todd Walter. Estimating long-term changes in actual evapotranspiration and water storage using a one-parameter model. *Journal of Hydrology* <In review>

likely to increase human dependence on some components of terrestrial water storage [*Taylor et al.,* 2013]. All the components of terrestrial water storage (henceforth referred to simply as "storage"), namely, groundwater, soil moisture, snow and surface reservoirs, are themselves susceptible to a variety of factors including changes in climate [e.g. *Döll, P.*, 2009; *Seneviratne et al.*, 2010; *Trenberth KE*, 2011; *Taylor et al.*, 2013], land cover (e.g.[e.g. *Nosetto et al.*, 2012; *Wang et al.*, 2012], and direct human use [*Rodell et al.*, 2009; *Famiglietti et al.*, 2011]. They may also have important feedback effects on climate [e.g. *Seneviratne et al.*, 2010].

Sustainable management of water resources would be aided considerably by an understanding of long-term patterns of storage variability and its responses to a variety of climate forcings. Yet long-term records of storage are sparse in most regions. Even in regions with active monitoring programs, data cover only a few decades and there is considerable uncertainty about the reliability of regional extrapolations from point or sub-regional data. The difficulty in generating long records of water storage is intimately related to the difficulty of estimating another key component of the terrestrial water balance: evapotranspiration, resulting in a one equation- two unknown quantities problem.

Over the past decade, the Gravity Recovery and Climate Experiment (GRACE) has generated data on regional changes in terrestrial water storage. Data from GRACE have been used to characterize changes in water storage in many regions across the world [e.g. *Crowley et al.*, 2006; *Rodell et al.*, 2007, 2009; *Famiglietti et al.*, 2011]. Because GRACE data have existed only for a decade, many applications of GRACE data have tended to focus on this period. However, when combined with models, these data have potential in extending the understanding of hydrologic patterns beyond the period of their record. Some studies have used GRACE data to

calibrate elaborate models [e.g. *Werth et al.*, 2009; *Werth and Güntner*, 2010; *Sun et al.*, 2012; *Xie et al.*, 2012; *Qiao et al.*, 2013]. Here we show that GRACE data can be used in combination with a one-parameter model to estimate long-term patterns of evaporanspiraton and "active" storage.

The simple model used in this study is based on the assumption that evapotranspiration (E) approaches potential evapotranspiration (E_o) asymptotically with increasing active storage [*Tuttle and Salvucci*, 2012]. The one parameter in the model determines how rapidly the E approaches the E_o with increasing storage. The advantage of this parsimonious approach is that it is simple and gives reasonable estimates of storage variations without the need for many data other than precipitation, maximum and minimum temperatures, elevation, and river discharge. The model's simplicity also makes it very transparent, consistent with the "behavioral" modeling approach proposed by [*Schaefli et al.*, 2011] for investigating hydrology-climate change interactions. The objective of this study is to demonstrate the utility of this approach to extending the water storage time series in the Missouri river basin. We use these modeled estimates of storage and E to evaluate long term trends (1929 – 2012) in the hydrologic budget.

Model Description

We use the standard watershed water budget:

$$\Delta S = P - Q - E \quad (1)$$

where E is the evapotranspiration, P is the precipitation, Q is the discharge, and ΔS is the change in storage (all in units of depth per time). We assume that there are reasonably good P and Q data

but ΔS and E are typically unknown. As described below, we reduced E to a one parameter function.

The ratio of E to E_o can be modeled as a function of storage [*Tuttle and Salvucci*, 2012]

$$\beta = 1 - e^{-\alpha S} \tag{2}$$

where $\beta = E/E_o$, α is an empirical parameter, and S is the active storage. Although not theoretically proven, this relationship has the intuitive appeal of E asymptotically approaching E_o as storage increases. E is a function of many different factors [*Brutsaert*, 1982], however, with only one parameter to calibrate, this equation has the advantage of parsimony. Moreover, it can be argued that α, which determines how rapidly β approaches 1, captures most of these variations over a sufficiently large temporal and spatial scale.

Potential evapotranspiration was calculated on a daily time step for each Global Historical Climate Network (GHCN) station. The Priestley-Taylor method [*Priestley and Taylor*, 1972] was used, i.e.

$$E_0 = \alpha_e \frac{\Delta}{\Delta+\gamma}(R_n - G) \tag{3}$$

where α_e is the Priestley-Taylor constant, assumed here to be 1.26, Δ is the slope of the saturated vapor pressure curve at the mean temperature of the day, γ is the psychrometric constant, R_n is the net incoming radiation, and G is the ground heat flux, assumed to be negligible at this time step [*Allen et al.*, 1988]. As the psychrometric constant, γ, is dependent on pressure:

$$\gamma = \frac{c_p P}{\varepsilon\lambda} = 0.665 \times 10^{-3} p \tag{4}$$

where γ is in kPa°C^{-1} , c_p is the specific heat at constant pressure (1.013×10^{-3}MJ kg^{-1} °C^{-1}), p is pressure (kPa), ε is the ratio of molecular weights of water vapor to dry air (0.622) and λ is the latent heat of vaporization (2.45 MJ kg^{-1}). Pressure for each station is calculated based on elevation using a simplification of the ideal gas law:

$$p = 101.3\left(\frac{293-0.0065z}{293}\right)^{5.26} \quad (5)$$

where p is the pressure (kPa) and z the elevation above sea level (m) [*Allen et al.*, 1988]. The p calculated this way for each station corresponded well with the mean pressure recorded at each station in the Global Summary of Day (GSOD) database.

The net radiation was calculated using the method described by Walter et al. [2005] and Archibald and Walter [2013, 2014]. The EcoHydRology R package [*Fuka et al.*, 2013] was used to build this model with modifications to γ as stated above.

Data and Methods

Climate variables were obtained from the GHCN [*Vose et al.*, 1992], except where mentioned from the GSOD database (http://www.climate.gov/global-summary-day-gsod). Daily discharge data were obtained from the United States Geological Service (USGS) gauge number 06934500 at Hermann, MO. GRACE data, used to estimate changes in storage for the period beginning January 2003, were obtained in the form of monthly grids of equivalent water thickness from http://grace.jpl.nasa.gov/data/gracemonthlymassgridsland/ [*Swenson and Wahr*, 2006; *Landerer and Swenson*, 2012]. The GRACE satellites detect changes in Earth's gravitational field which

may be caused by a number of factors apart from changes in storage. The 1° gridded data used here were pre-processed to remove the effect of the post-glacial rebound signal as well as of atmospheric and oceanic effects. The gridded data also take into account the "stripes" that are an artifact of the processing. The dataset used here is derived from the spherical harmonic coefficient dataset generated by GRACE using 200 km Gaussian filter and a degree cutoff of 60 for the gravity field solutions. Locations of the GHCN and USGS gauges as well as the boundaries of the basin are shown in Fig. 2.1.

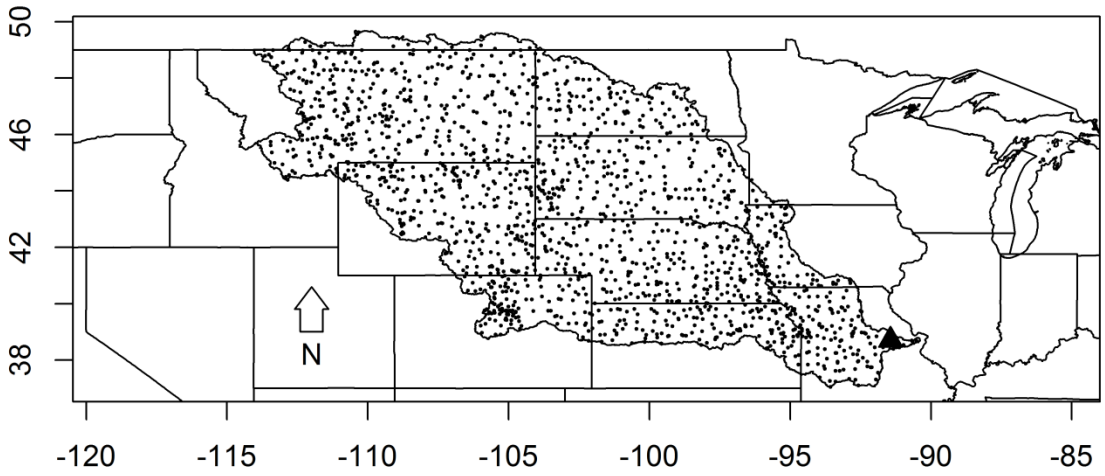

Figure 2.1: Map of the Missouri river basin and GHCN stations (points) and USGS discharge station (triangle, bottom right) used in this study.

Daily E_o and precipitation were first aggregated for each station to a pentad (five day) time step and then interpolated over the river basin using the inverse distance weighting method with an

exponent of 2 [*Brutsaert*, 2005]. For stations with 1 day or less of missing data for the pentad, it was assumed that the E_o or P would be reflected adequately by the mean value of the rest of the days. If more than one day of data were missing, that station was ignored for that pentad. There are 1,731 GHCN stations in the Missouri river basin (Fig. 2.1).

We calculated ΔS from October 1928 to June 2013 using exhaustive combinations of α (from 0.001 cm^{-1} to 0.5 cm^{-1} in increments of 0.001 cm^{-1}) and initial S (from 0 to 100 cm in increments of 1 cm). The ΔS at each time step was estimated from Eq. 1. The ΔS obtained at each time step was added to the storage at that time step in order to produce the storage for the subsequent time step. Any time series in which S was negative at any point was neglected since it is physically impossible to have negative storage; that some time series would have negative S is unsurprising since we do not initially constrain combinations of α and S except by specifying the ranges mentioned above.

The most likely values of α and S were selected on the basis of the residual sum of squares (*SSR*) between S anomalies and ΔS from GRACE and the modeled values:

$$SSR_{S'} = \sum_{i=1}^{i=n} \left(S'_{GRACE_i} - S'_{mod_i}\right)^2 \ldots \quad (6)$$

$$SSR_{\Delta S} = \sum_{i=1}^{i=n} \left(\Delta S_{GRACE_i} - \Delta S_{mod_i}\right)^2 \ldots \quad (7)$$

where S'_{GRACE} denotes storage anomalies from GRACE data (with respect to the January 2003 to June 2013 time period), S'_{mod} denotes storage anomalies from the modeled time, ΔS_{GRACE} denotes change in storage from GRACE data, ΔS_{mod} denotes change in storage from the

modeled time series, and GRACE series and n is the number of GRACE data points in the time period January 2003 to June 2013.

Since the estimated values are in time steps of pentads, estimated S is first interpolated to the GRACE time periods to obtain the S anomaly (S'_{mod}) and ΔS series (ΔS_{mod}) with the same time periods as the GRACE time series. The model was fed ten years of mean weather (climatological) and discharge data in order to allow it to "spin-up."

Long-term (1929-2012) trends were estimated using the non-parametric Theil-Sen method in the wq R package [*Jassby and Cloern*, 2012]. All computations were performed in R [*R Core Team*, 2012]. More intensive computations, such as spatial interpolation of climate data, were performed using the computational facilities at the National Center for Atmospheric Research [*Computational and Information Systems Laboratory*, 2012].

Results and Discussion

For this basin, streamflow is an order of magnitude smaller than the other fluxes in Eq. 1. For a few months in the late-fall to early-spring (ONDJFM), E estimated from Eq. 1 and GRACE data is either negative or greater than the E_o. Most were in NDJF when both E and E_o are both very small, and therefore this is likely to be an artifact of the error associated with each of the variables in Eq. 1. Despite the high degree of relative variability in the late fall to early spring, the values of "observed" β tend to be much more constrained in the late spring-early fall (AMJJAS), when they range between 0.23 and 0.85, with ~75% of these values between 0.4 and 0.65.

The two methods (Eqs. 6 and 7) give very similar results in most respects (Table 2.1, Figs. 2 and A2.1), although the mean *S* predicted by the $SSR_{S'}$ method has a narrower range. The *S* predicted here is similar to the values obtained by Tuttle and Salvucci [2012] (see their Fig. 4). Although the size and location of the watersheds are different, the similarity of the estimates provides further confidence in these results. While α and *S* values vary over a factor of two, this does not result in a big difference in the predicted values of changes in storage and storage anomalies which are the main points of interest in this study (Fig. 2.2). The high degree of correlation with GRACE data (Figs. 2.2 and A2.1) as well as the narrow distribution of the results indicate the usefulness of this parsimonious approach.

Table 2.1: Values of α (cm^{-1}), mean storage $\bar{S}$ (cm) and Pearson's product moment correlation (*r*) obtained by the two methods

	$SSR_{S'}$	$SSR_{\Delta S}$
α (minimum *SSR*)	0.029	0.028
α range (*SSRs* within 5% of minimum)	0.022 - 0.038	0.018 - 0.040
$\bar{S}$ (minimum *SSR*)	23.4	22.6
$\bar{S}$ range (*SSRs* within 5% of minimum)	17.6 - 29.5	16.8 - 35.9
r between modeled and observed *S'* (minimum *SSR*)	0.79	0.79
r between modeled and observed *S'* (*SSRs* within 5% of minimum)	0.76 – 0.81	0.76 – 0.82
r between modeled and observed ΔS (minimum *SSR*)	0.87	0.87
r between modeled and observed ΔS anomalies (*SSRs* within 5% of minimum)	0.87 – 0.88	0.87 – 0.88

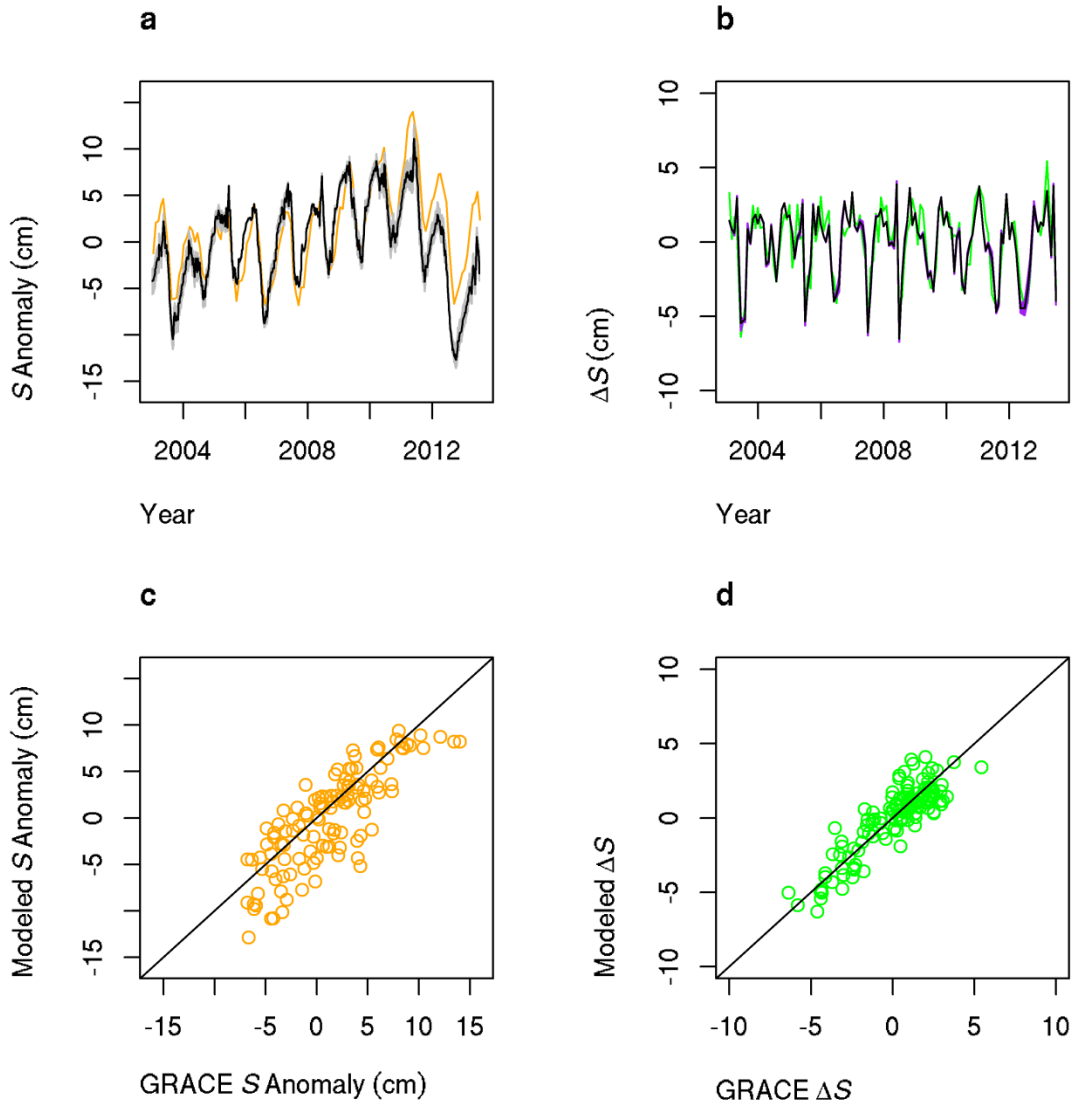

Figure 2.2: Modeled and GRACE data found by minimizing $SSR_{S'}$: (a) S anomalies plotted as a time series; black lines are GRACE data; orange lines are the best (lowest *SSR*) modeled data, and gray lines are other modeled data within 5% of the lowest *SSR*. (b) ΔS plotted as a time series; black lines are GRACE data; green lines are the best (lowest *SSR*) modeled data, and purple lines (barely visible) are other modeled data within 5% of the lowest *SSR*. (c) S anomalies, modeled (best (lowest *SSR*) modeled data) v. observed, and (d) ΔS, modeled (best (lowest *SSR*) modeled data) v. observed. In (c) and (d), lines shown to facilitate comparison have intercept = 0 and slope = 1. Plots for minimum $SSR_{\Delta S}$ are shown in Figure A2.1.

Long term (1929-2012) annual time series of P, Q, E_o, and model-estimated E and ΔS are shown in Fig. 2.3. P, Q and E have increased (Table 2.2, Fig. 2.3) but ΔS does not show a significant ($p < 0.05$) trend. Increase in E at regional and global scales has been suggested in many previous studies [e.g. *Brutsaert and Parlange*, 1998; *Milly and Dunne*, 2001; *Szilagyi et al.*, 2001; *Walter et al.*, 2004; *Brutsaert*, 2006]. Brutsaert and Parlange [1998] suggested that global decreases in pan evaporation can be explained by an increase in actual E because of the Bouchet-Morton "complementary relationship." In this study, E_o has not changed, while E has increased. Thus the apparent potential evaporation term, the quantity often assumed to be measured by pan evaporation, has, in effect, decreased, supporting Brutsaert and Parlange [1998]. The increasing trend in E of 0.055 cm y^{-2} seen in this study is of the same order of magnitude obtained in other studies. Brutsaert [2006] found a global trend in E of 0.044 cm y^{-2} for 1950-2000. Milly and Dunne [2001] and Walter et al. [2004] found trends in E equivalent to 0.069 (1949-1997) and 0.11 (1950-2000) cm y^{-2} for the Mississippi river basin, of which the Missouri is a sub-basin. These studies also found somewhat higher trends for precipitation, 0.178 cm y^{-2} [*Milly and Dunne*, 2001] and 0.176 cm y^{-2} [*Walter et al.*, 2004] than the trend of 0.084 cm y^{-2} found in this study, indicating a spatial variation in the trends within the Mississippi basin, i.e., other parts of the Mississippi basin have larger increases in E than in the Missouri River sub-basin..

Since E_o has not increased significantly (Table 2.2), the increase in E is driven by the increase in water availability from increased precipitation. Although there is no significant trend in the ΔS, there is a significant positive trend in S' (Table 2.2, Fig. 2.4). This may at first seem paradoxical but may be resolved as follows. The change in storage, ΔS, is in the difference between the flux terms P, Q and E. However the storage itself is a result of the integration of these flux terms over

time. By comparing the slopes of cumulative *P*, *Q* and *E*, one gets a value of change in storage

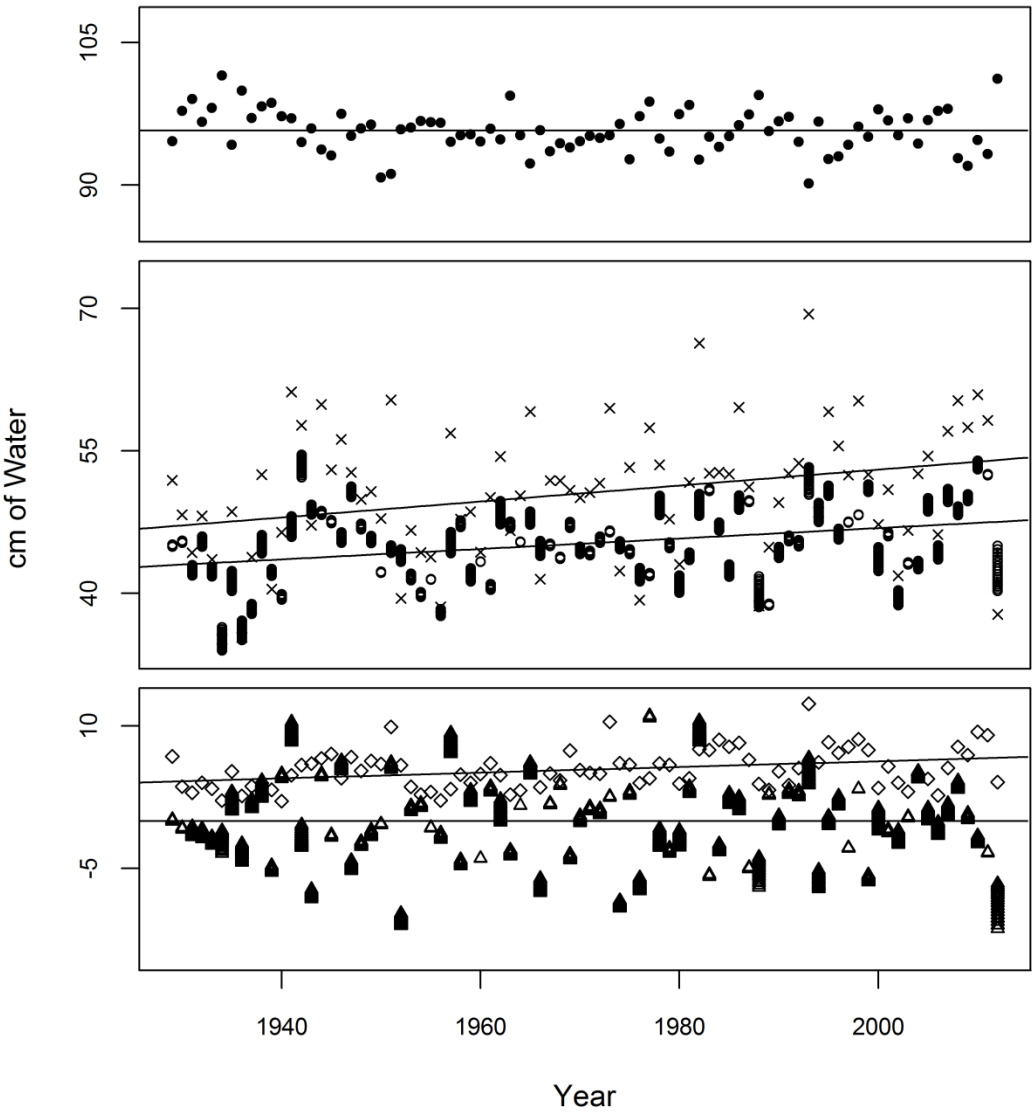

Figure 2.3: Potential evapotranspiration (E_o, closed circles) Annual precipitation (*P*, crosses), evapotranspiration (*E*, open circles), discharge (*Q*, open diamonds), and change in storage (ΔS, triangles) for 1929 – 2012. Note 1928 and 2013 were left out of trend analysis since data are incomplete for these years. The *E* and ΔS values plotted are for all time series with $SSR_{S'}$ within 5% of the minimum $SSR_{S'}$. Lines show slopes of each variable (values in Table 2.2); E_o and ΔS slopes shown are 0, since they do not have a significant trend.

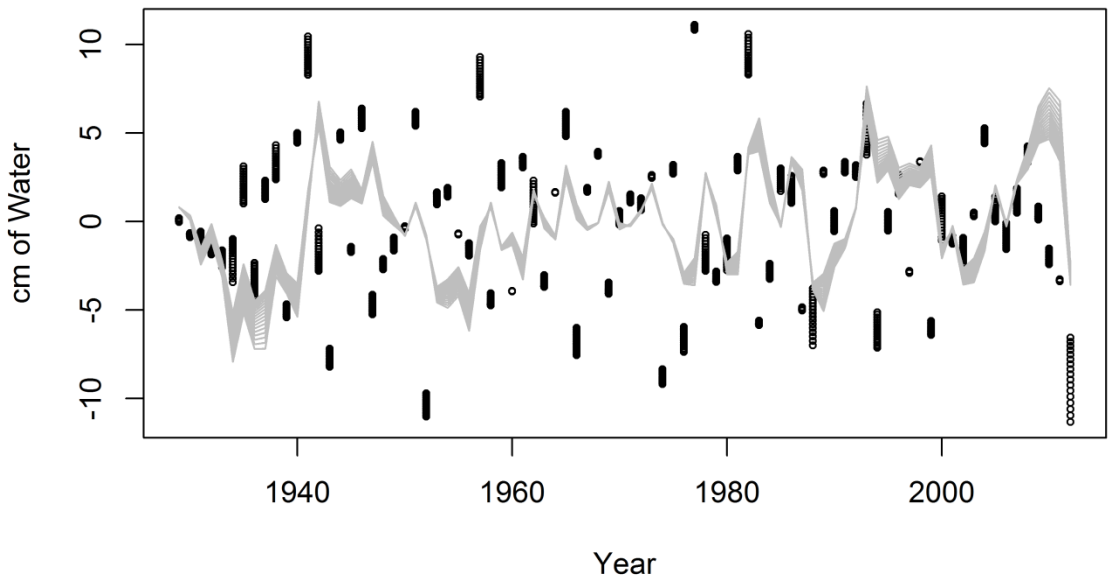

Figure 2.4: Annual change in storage (ΔS, black circles) and storage anomalies (S', gray lines) for 1929 – 2012. Note 1928 and 2013 were left out of trend analysis since data are incomplete for these years. The ΔS and S values plotted are for all time series with $SSR_{S'}$ within 5% of the minimum $SSR_{S'}$.

(0.064 cm y^{-1}) over this period that is close to the trend in the modeled S (~0.043 cm y^{-1}). This trend is an order of magnitude greater than the 0.008 cm y^{-1} (1965-2000) trend in groundwater storage that Brutsaert [2008] found for Illinois using long-term well data and recession slope analysis. While the magnitudes are not comparable because of the different "quantities" measured as well as the spatial differences, there is a concurrence among these studies that storage is increasing in this region. Note that the number of weather stations has varied over the years, with only 427 and 520 stations having at least 90% of the necessary data for P and E_o estimates, respectively. Using only the data from these stations with long-term records results in

trends of the same sign but larger magnitudes. The more conservative results obtained from using all the stations available at any given time are reported here.

Often, because of the lack of storage data, studies make the assumption that change in storage is negligible [e.g. *Walter et al.*, 2004]. In this particular region, the assumption that E may be estimated by the difference in P and Q is valid and suggests a trend very similar to the modeled estimate. However, this study highlights a nuance that is often overlooked in long-term hydrological studies. It is seen here that a significant (p-value < 0.05) trend in storage may be accompanied by no significant trend in year to year change in storage (Table 2). Usually the change in storage is very small compared to other quantities, however, the implications of the assumption that change in storage is negligible requires careful consideration. *Wang and Alimohammadi* [2012] found that especially under water-limited conditions, evapotranspiration may be overestimated if change in storage is neglected. This study provides a simple approach to incorporating changes in storage with limited data.

The increase in fluxes in this region is consistent with other evidence that suggests that the hydrological cycle is intensifying [*Huntington*, 2006] . The use of this method is limited by the resolution of the GRACE data, which allows its application only for relatively large river basins. However, this limitation may be addressed by future missions, and even the current resolution provides information on long term regional trends which may be supplemented by studies at smaller scales. Further study is also needed on the nature of the parameter α, and whether it is indeed constant for a given location.

Table 2.2: Trends in fluxes and slopes of cumulative terms. For *S*, the quantity in the "fluxes" column is ΔS, and in the cumulative terms column, it is the slope of the storage anomaly (S'). For *E*, ΔS and S', slopes given are the median values for all time series which had SSRs within 5% of the minimum SSR. In most cases, the median values for the $SSR_{S'}$ and $SSR_{\Delta S}$ methods were the same. Asterisks (*) indicate significant slopes ($p < 0.05$).

	Trends in fluxes (cm y^{-2})	Slope of cumulative terms (cm y^{-1})
P	0.084*	50.75*
Q	0.030*	5.48*
E_o	-0.017	95.44
E	0.055*	45.21*
ΔS	-0.001	0.042*($SSR_{S'}$); 0.043* ($SSR_{\Delta S}$)

Conclusions

Estimating patterns in storage and evapotranspiration are important steps to understanding the hydrological cycle. This study presents a simple method to estimate changes in these quantities for a large river basin. Given the simplicity of the model, and the errors inherent in the estimation of its inputs (such as *P*, E_o, *Q* and Δ*S*), it performs remarkably well. We used this model to show long term increases in *E* and storage in the Missouri river basin, consistent with other studies which have shown the intensification of the hydrological cycle.

References

Allen, R. G., L. S. Pereira, D. Raes, and M. Smith (1988), *Crop evapotranspiration - Guidelines for computing crop water requirements - FAO Irrigation and drainage paper 56*, Food and Agriculture Organization of the United Nations.

Brauman, K. A., G. C. Daily, T. K. Duarte, and H. A. Mooney (2007), The Nature and Value of Ecosystem Services: An Overview Highlighting Hydrologic Services, *Annu. Rev. Environ. Resour.*, *32*(1), 67–98, doi:10.1146/annurev.energy.32.031306.102758.

Brutsaert, W. (1982), *Evaporation into the Atmosphere*, Environmental Fluid Mechanics, Springer Netherlands.

Brutsaert, W. (2005), *Hydrology: An Introduction*, Cambridge University Press.

Brutsaert, W. (2006), Indications of increasing land surface evaporation during the second half of the 20th century, *Geophys. Res. Lett.*, *33*(20), L20403, doi:10.1029/2006GL027532.

Brutsaert, W. (2008), Long-term groundwater storage trends estimated from streamflow records: Climatic perspective, *Water Resour. Res.*, *44*(2), W02409, doi:10.1029/2007WR006518.

Brutsaert, W., and M. B. Parlange (1998), Hydrologic cycle explains the evaporation paradox, *Nature*, *396*(6706), 30–30, doi:10.1038/23845.

Computational and Information Systems Laboratory (2012), *Yellowstone: IBM iDataPlex System (University Community Computing)*, National Center for Atmospheric Research, Boulder, Colorado.

Crowley, J. W., J. X. Mitrovica, R. C. Bailey, M. E. Tamisiea, and J. L. Davis (2006), Land water storage within the Congo Basin inferred from GRACE satellite gravity data, *Geophys. Res. Lett.*, *33*(19), L19402, doi:10.1029/2006GL027070.

Döll, P. (2009), Vulnerability to the impact of climate change on renewable groundwater resources: a global-scale assessment, *Environ. Res. Lett.*, *4*(3), 035006.

Famiglietti, J. S., M. Lo, S. L. Ho, J. Bethune, K. J. Anderson, T. H. Syed, S. C. Swenson, C. R. de Linage, and M. Rodell (2011), Satellites measure recent rates of groundwater depletion in California's Central Valley, *Geophys. Res. Lett.*, *38*(3), L03403, doi:10.1029/2010GL046442.

Fuka, D., M. T. Walter, J. A. Archibald, T. S. Steenhuis, and Z. M. Easton (2013), *A community modeling foundation for Eco-Hydrology*.

Huntington, T. G. (2006), Evidence for intensification of the global water cycle: Review and synthesis, *J. Hydrol.*, *319*(1–4), 83–95, doi:10.1016/j.jhydrol.2005.07.003.

Jassby, A., and J. E. Cloern (2012), Exploring water quality monitoring data,

Landerer, F. W., and S. C. Swenson (2012), Accuracy of scaled GRACE terrestrial water storage estimates, *Water Resour. Res.*, *48*(4), W04531, doi:10.1029/2011WR011453.

Milly, P. C. D., and K. A. Dunne (2001), Trends in evaporation and surface cooling in the Mississippi River Basin, *Geophys. Res. Lett.*, *28*(7), 1219–1222, doi:10.1029/2000GL012321.

Nosetto, M. D., E. G. Jobbágy, A. B. Brizuela, and R. B. Jackson (2012), The hydrologic consequences of land cover change in central Argentina, *Ecosyst. Serv. Land-Use Policy*, *154*(0), 2–11, doi:10.1016/j.agee.2011.01.008.

Priestley, C. H. B., and R. J. Taylor (1972), On the Assessment of Surface Heat Flux and Evaporation Using Large-Scale Parameters, *Mon. Weather Rev.*, *100*(2), 81–92, doi:10.1175/1520-0493(1972)100<0081:OTAOSH>2.3.CO;2.

Qiao, L., R. B. Herrmann, and Z. Pan (2013), Parameter Uncertainty Reduction for SWAT Using Grace, Streamflow, and Groundwater Table Data for Lower Missouri River Basin1, *JAWRA J. Am. Water Resour. Assoc.*, *49*(2), 343–358, doi:10.1111/jawr.12021.

R Core Team (2012), *R: A language and environment for statistical computing.*, R Foundation for Statistical Computing, Vienna, Austria.

Rodell, M., J. Chen, H. Kato, J. Famiglietti, J. Nigro, and C. Wilson (2007), Estimating groundwater storage changes in the Mississippi River basin (USA) using GRACE, *Hydrogeol. J.*, *15*(1), 159–166, doi:10.1007/s10040-006-0103-7.

Rodell, M., I. Velicogna, and J. S. Famiglietti (2009), Satellite-based estimates of groundwater depletion in India, *Nature*, *460*(7258), 999–1002, doi:10.1038/nature08238.

Schaefli, B., C. J. Harman, M. Sivapalan, and S. J. Schymanski (2011), HESS Opinions: Hydrologic predictions in a changing environment: behavioral modeling, *Hydrol. Earth Syst. Sci.*, *15*(2), 635–646, doi:10.5194/hess-15-635-2011.

Seneviratne, S. I., T. Corti, E. L. Davin, M. Hirschi, E. B. Jaeger, I. Lehner, B. Orlowsky, and A. J. Teuling (2010), Investigating soil moisture–climate interactions in a changing climate: A review, *Earth-Sci. Rev.*, *99*(3–4), 125–161, doi:10.1016/j.earscirev.2010.02.004.

Sun, A. Y., R. Green, S. Swenson, and M. Rodell (2012), Toward calibration of regional groundwater models using GRACE data, *J. Hydrol.*, *422–423*(0), 1–9, doi:10.1016/j.jhydrol.2011.10.025.

Swenson, S., and J. Wahr (2006), Post-processing removal of correlated errors in GRACE data, *Geophys. Res. Lett.*, *33*(8), L08402, doi:10.1029/2005GL025285.

Szilagyi, J., G. G. Katul, and M. B. Parlange (2001), Evapotranspiration intensifies over the conterminous United states, *J. Water Resour. Plan. Manag.*, *127*(6), 354–362.

Taylor, R. G. et al. (2013), Ground water and climate change, *Nat. Clim. Change*, *3*(4), 322–329, doi:10.1038/nclimate1744.

Trenberth KE (2011), Changes in precipitation with climate change, *Clim. Res.*, *47*(1-2), 123–138.

Tuttle, S. E., and G. D. Salvucci (2012), A new method for calibrating a simple, watershed-scale model of evapotranspiration: Maximizing the correlation between observed streamflow

and model-inferred storage, *Water Resour. Res.*, *48*(5), W05556, doi:10.1029/2011WR011189.

Vose, R. S., R. L. Schmoyer, P. M. Steurer, T. C. Peterson, R. Heim, T. R. Karl, and J. K. Eischeid (1992), *The Global Historical Climatology Network: Long-term monthly temperature, precipitation, sea level pressure, and station pressure data*, Technical Report, Oak Ridge National Lab., TN (United States). Carbon Dioxide Information Analysis Center.

Walter, M. T., D. S. Wilks, J.-Y. Parlange, and R. L. Schneider (2004), Increasing Evapotranspiration from the Conterminous United States, *J. Hydrometeorol.*, *5*(3), 405–408, doi:10.1175/1525-7541(2004)005<0405:IEFTCU>2.0.CO;2.

Wang, D., and N. Alimohammadi (2012), Responses of annual runoff, evaporation, and storage change to climate variability at the watershed scale, *Water Resour. Res.*, *48*(5), W05546, doi:10.1029/2011WR011444.

Wang, S., B. J. Fu, G. Y. Gao, X. L. Yao, and J. Zhou (2012), Soil moisture and evapotranspiration of different land cover types in the Loess Plateau, China, *Hydrol. Earth Syst. Sci.*, *16*(8), 2883–2892, doi:10.5194/hess-16-2883-2012.

Werth, S., and A. Güntner (2010), Calibration analysis for water storage variability of the global hydrological model WGHM, *Hydrol. Earth Syst. Sci.*, *14*(1), 59–78, doi:10.5194/hess-14-59-2010.

Werth, S., A. Güntner, S. Petrovic, and R. Schmidt (2009), Integration of GRACE mass variations into a global hydrological model, *Earth Planet. Sci. Lett.*, *277*(1–2), 166–173, doi:10.1016/j.epsl.2008.10.021.

Xie, H., L. Longuevergne, C. Ringler, and B. R. Scanlon (2012), Calibration and evaluation of a semi-distributed watershed model of Sub-Saharan Africa using GRACE data, *Hydrol. Earth Syst. Sci.*, *16*(9), 3083–3099, doi:10.5194/hess-16-3083-2012.

CHAPTER 3

Using autoregression to model persistence in climatic time series[3]

Chapter Summary

A number of studies have examined the persistence of various hydrological and climatological time series. However, it is not always clear what stochastic, leave alone physical, processes can generate these persistence patterns. Here we show that different degrees of persistence in a time series may be modeled using a simple autoregressive approach. We model precipitation, temperature, potential evapotranspiration a drought index for the 20th century using this approach. We demonstrate that the number of non-zero autoregression coefficients does not affect the degree of persistence. However, autoregression coefficients may provide some insights into the physical processes affecting the time series.

Introduction

Since Hurst [1950] discovered the existence of long-range persistence of flows in the Nile, there has been an interest in examining the same phenomenon in various hydrological [e.g. *Matsoukas et al.*, 2000], atmospheric [e.g. *Alvarez-Ramirez et al.*, 2011], and other time series. The physical processes that lead to persistence in a climatic time series are not yet clear. For example, *Klemes* [1974] showed that the Hurst "phenomenon" could be explained by multiple factors. Some

[3] Asha N. Sharma, Calum G. Turvey, M. Todd Walter and Michael F. Walter. Using autoregression to model persistence in climatic time series <Internal review>

studies [e.g. *Bierkens and van den Hurk*, 2007] have tested hypotheses on feedback mechanisms using models, with the Hurst exponent used as a measure of persistence. Apart from the important question of physical processes that lead to particular persistence characteristics, it is not even always clear what stochastic processes might generate it. Here we show that different degrees of persistence in various climatic time series may be explained through a simple autoregressive approach, and that this leads to some interesting insights into stochastic patterns associated with persistence.

The approach we take in this study builds on previous work by Wongsasutthikul and Turvey [2011]. See their paper for a full derivation of the proofs; Here we briefly summarize here their key results. They show that the sum of coefficients in an autoregressive (AR) process being equal to one implies the presence of a unit root. Let Y_t be an AR process of order q (AR(q)). Thus

$$Y_t = a_1 Y_{t-1} + a_2 Y_{t-2} + ... + a_q Y_{t-q} + \varepsilon_t \quad (1)$$

where a_i are cofficients and ε_t is an innovation (i.e. "error") term that follows a Gaussian If $\sum_{i=1}^{q} a_i = 1$, then

$$a_q = 1 - \sum_{i=1}^{q-1} a_i \quad (2)$$

The characteristic polynomial for the roots ν of AR(q) is

$$\nu^q - \sum_{i=1}^{q-1} a_i \nu^{q-i} - a_q = 0 \quad (3)$$

From Eqs. 2 and 3, we get

$$v^q - \sum_{i=1}^{q-1} a_i \left(v^{q-i} - 1\right) - 1 = 0 \tag{4}$$

This implies that $v = 1$ is a root. It can similarly be shown that the reverse also holds, i.e. $v = 1$ implies $\sum_{i=1}^{q} a_i = 1$. It can be shown that a process that has stationary increments will have $\sum_{i=1}^{q} a_i = 1$. The above finding implies that such a process has a unit root.

The Hurst exponent H is typically used to describe the persistence of a fractional Brownian motion $B^{(H)}$, which is a generalization of the Brownian motion to include fractional behavior. This process has the following properties [*Mandelbrot*, 1977; *Wongsasutthikul and Turvey*, 2011]:

1. $B^{(H)}(0) = 0$ and $E\,[B^{(H)}(t)] = 0$ for all $t \geq 0$.
2. $B^{(H)}$ has stationary increments.
3. $B^{(H)}$ has continuous trajectories.
4. $B^{(H)}$ is a Gaussian process.

It can be shown that it is possible to have an AR(q) process with all the above properties. Thus fractional Brownian motion, or a process with "persistence," can be modeled as an AR process. Also, as noted above, such an AR(q) process should have the sum of its coefficients be equal to one. According to the scaled variance ratio method [*Cannon et al.*, 1997; *Turvey*, 2007], the H for a time series can be calculated from:

$$\frac{E\left[Y(t+k) - Y(t)\right]^2}{E\left[Y(t+1) - Y(t)\right]^2} = \frac{\sigma_k^2}{\sigma_1^2} = \left(k\right)^{2H} \tag{5}$$

The relationship of this *H* to the AR process is given by:

$$H = \frac{\ln\left(k + \frac{2\sum_{i=1,j=1,i<j}^{k} Cov[Z_i, Z_j]}{\sum_{i=1}^{q} a_i^2 (E[Z_{i+1}^2] - E[Z_{i+1}]^2) + 2\sum_{i=1,j=1,i<j}^{q} a_i a_j (E[Z_{i+1}Z_{j+1}] - E[Z_{i+1}]E[Z_{j+1}]) + 2\sigma^2 - 2Cov[\varepsilon_t, \varepsilon_{t-1}]}\right)}{2\ln(k)} \quad (6)$$

where $Z_i = Y_t - Y_{t-i}$ and σ^2 is the variance of ε_t. It can be seen from this equation that if $Cov[Z_i, Z_j] = 0$ then *H* is 0.5. Positive and negative values of $Cov[Z_i, Z_j]$ will likewise give $H > 0.5$ and $H < 0.5$, respectively.

Here we examine if departures from expected values of four climatic time series, i.e. precipitation, temperature, potential evapotranspiration (PET) and the Standardized Precipitation Evapotranspiration drought index (SPEI) in a region roughly encompassing the conterminous US and Mexico follow an AR process of the kind described above. We then further explore what *H* implies in terms of other characteristics the time series. Finally, we compare the persistence patterns in the various time series to each other.

Methods

Monthly gridded (0.5°) precipitation, temperature, and PET data for 1901 to 2009 were obtained from the University of East Anglia Climatic Research Unit Time Series version 3.1[*CRU*, n.d.]. The PET data are based on the Food and Agriculture Organization (FAO) grass reference evapotranspiration equation, a variant of the Penman-Monteith equation [*Allen et al.*, 1988]. The Standardized Precipitation Evapotranspiration Index (SPEI) is a drought index based on Climate

Research Unit (CRU) precipitation and potential evapotranspiration data [*Vicente-Serrano et al.*, 2010a; *Beguería et al.*, 2010; *Vicente-Serrano et al.*, 2010b]. SPEI is a drought index that, like the commonly used Palmer Drought Severity Index (PDSI), takes into account not just the "supply" of water through precipitation but also the "demand" through evapotranspiration. The SPEI dataset is available at time scales between 1 month and 48 months for the years 1901-2011. The availability of the index at the 1 month time-scale is particularly useful in comparing its persistence patterns with those of monthly precipitation, temperature and PET.

The region selected for this study encompassed a box bounded by latitudes 15 °N and 50 °N, and longitudes 125 °W and 60 °W, which roughly encompasses the conterminous US and Mexico. This region was selected to allow for a range of climatic and geographic factors that might influence the processes that generate different degrees of persistence in the selected time series.

For each of the four different time series (P, T, PET and SPEI), departures from the "expected" values were estimated in a method similar to Kantelhardt et al. [*Kantelhardt et al.*, 2006]. The "expected" value for a particular location in a given month is estimated as the predicted value for that particular month based on a linear regression of the data from the entire time series of that month: For each location, the departure in a given month is the difference of observed and expected value for the month divided by the standard deviation of all values observed in that month of the year. For example, for precipitation P_{my} in month *m* and year *y*, the departure is:

$$d_{my} = \frac{P_{my} - \overline{P_m}}{\sigma_{Pm}} \quad (7)$$

where $\overline{P_m}$ is the mean precipitation for month m across all years, and σ_{Pm} is the standard deviation of precipitation for month m across all years. The departures are cumulatively summed to form a time series of cumulative departures:

$$D_{my} = \sum_{y=1901}^{y=2009} \sum_{m=1}^{m=12} d_{my} \quad (8)$$

where Y is the year. While most studies have focused on the "raw" time series, this is a useful measure physically because often it is the summation over time of departures rather than any particularly anomalous month that is of interest. This concept is similar conceptually to the idea of growing degree days, where the temperature difference with respect to some threshold value is cumulatively summed over time. Unrestricted autoregression was performed on each of these time series, with a maximum allowed lag of 36 months. I.e., first the time series D_{my} was denoted as Y_t with the only difference between the two being that while m and y indicate specific months and years, t only indicates the number of months since the start of the record. The "independent" terms in the autoregression were then $\alpha_1 Y_{t-1}$, $\alpha_2 Y_{t-2}$,… $\alpha_{36} Y_{t-36}$. where α_1 , α_2,… α_{36} are the AR coefficients and Y_{t-1} , Y_{t-2},… Y_{t-36} are referred to henceforth as the lags. As in other kinds of regression, not all of the independent variables or lags, need be significant. The time series were also subjected to a restricted autoregression, using only the significant ($p < 0.05$) lags with the restriction that the sum of the coefficients be equal to one.

Since Hurst's original work, several methods to calculate the Hurst exponent have been proposed. Here, persistence was estimated using the scaled variance ratio (SVR) technique shown in Eq.5 [*Turvey*, 2007; *Wongsasutthikul and Turvey*, 2011]. Since many recent studies [e.g. *Matsoukas et al.*, 2000; *Kantelhardt et al.*, 2006] have used detrended fluctuation analysis [*Peng et al.*, 1994] to estimate persistence, we also used this method and compared results to

those obtained using the SVR technique. The analysis was performed using the R programming language [*R Core Team*, 2013] and the computational facilities at US National Center for Atmospheric Research [*Computational and Information Systems Laboratory*, 2012].

Results and Discussion

The sum of the unconstrained autoregressions was close to 1 for all the points in the selected area (Fig. 3.1) and for all the time series. These values suggest the existence of a unit root, however a restricted regression was done to verify this. The restricted autoregression was performed by selecting only the significant lags ($p < 0.05$) from the unrestricted autoregression, with the constraint that their sum be equal to one. Model comparison was done with the Bayes Information Criterion (BIC), which is lower for the "better" model. An absolute difference of less than 2 points is considered to be non-significant, while absolute differences greater than 2 are considered to be significant. For each time series, between 0.6 – 2.1% of the gridpoints have a BIC difference of the restricted and unrestricted models within 2 points, i.e. in the range in which the models are not considered significantly different (Fig. A3.1 in supplement). Between 97 and 98.9 % of the grid points have restricted models with BICs more than 2 points lower than for the unrestricted models. Since the BIC is a criterion that balances goodness of fit with number of parameters, this result suggests that the restricted models may even be better than the unrestricted ones. AR models are sometimes used to model climatological and hydrological time series [*McKenney et al.*, 2006; *Triacca et al.*, 2014], although often more complicated models are used. Our results indicate that AR models can indeed be used to realistically simulate the persistence found in hydroclimatology, provided that the sum of the coefficients be equal to one.

Otherwise, the model will explode, i.e., the sum of the deviations will continue to increase or decrease or collapse to zero. The coefficients may be made to sum to one by allowing the model to choose a higher maximum order since larger lags may have a small but significant impact on the time series.

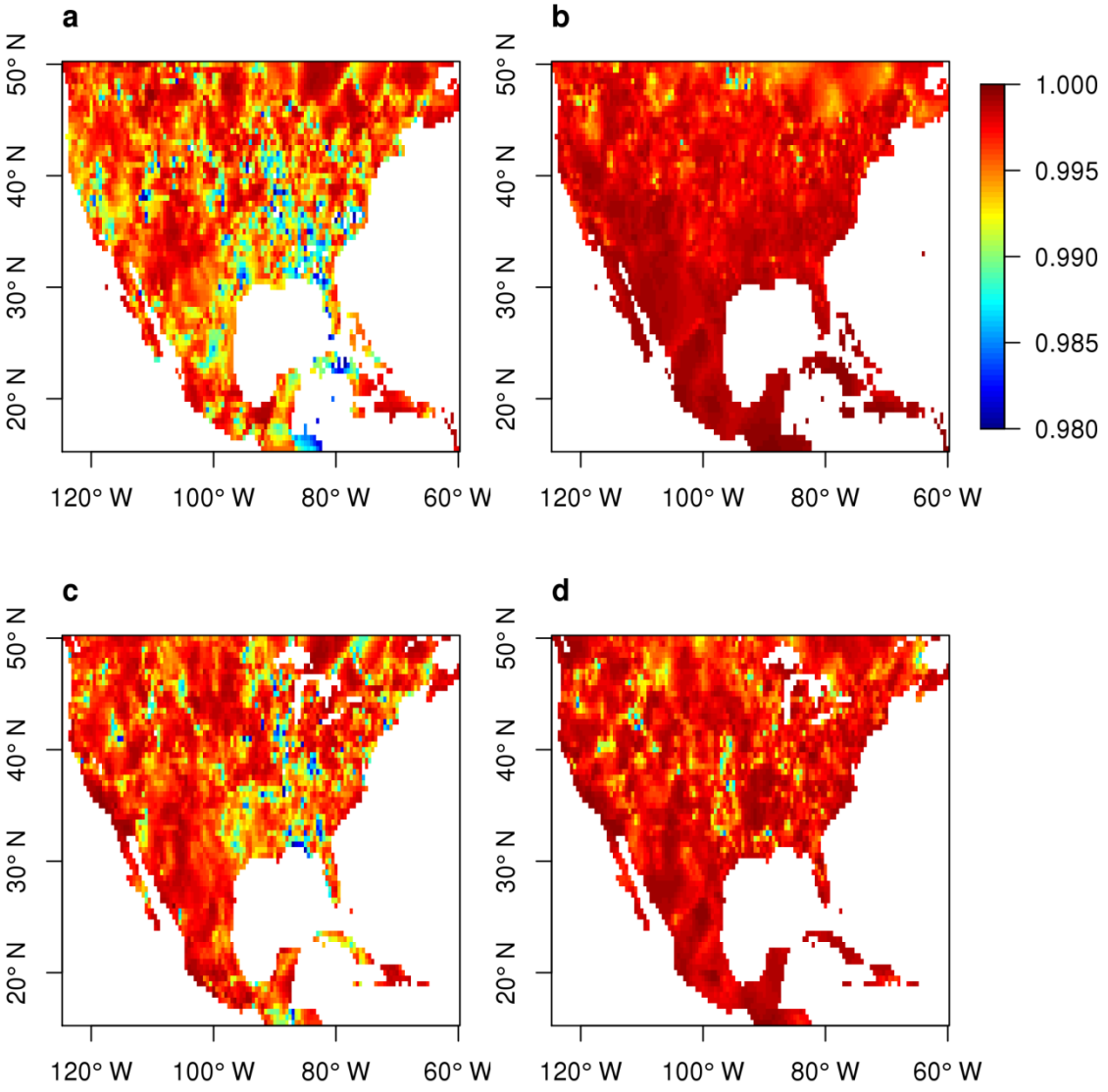

Figure 3.1: Sum of coefficients for unrestricted autoregressive model: (a) Precipitation, (b) Temperature, (c) SPEI, (d) PET.

As discussed earlier, that the sum of the autoregression coefficients equals to one points to the existence of a unit root in the time series. Typically in the literature the existence of a unit root is immediately taken as proof of non-stationarity in the time series[*Wongsasutthikul and Turvey*, 2011]. However, Wongsasutthikul and Turvey [2011] show that if a process has stationary but not necessarily independent increments, it will have a unit root. In our case, the increments are the departures of the variable (P, T, PET, or SPEI) from its expected value (as defined by Eq. 7), which implies that, while they may not be independent, they are stationary. In other words, there is no evidence in these time series to suggest an increase in variance of the departures. Increase in variability of precipitation and temperature is predicted by climate models [*IPCC*, 2013]. Some authors have found trends in the variability of precipitation over the last century [*Tsonis*, 1996], e.g. Sun [2012] found a decrease in global monthly precipitation variability but an increase in variability over the United States. Karl et al. [*Karl et al.*, 1995] found no significant trends in monthly temperature variability over the United States. We find no evidence for trends in the variability of departures of either temperature or precipitation. Note that this need not indicate that the extremes are not getting more extreme: we take into account the trend in the mean, and therefore, the highest and lowest values attainable given the same standard deviation would be higher and lower, respectively, than if the mean had not changed. Additionally, there may be trends in daily variability which may not be reflected in the monthly record. This is also seen in Karl et al. [1995].

The Hurst exponents of the time series were estimated by two methods: the scaled variance ratio method (Fig. 3.2) and the detrended fluctuation analysis (Fig. A3.2). Both these methods show remarkably similar results in terms of the spatial patterns of persistence. In general it is seen that while precipitation and SPEI do show persistence, the majority of the region experiences, at

most, a moderate degree of persistence with *H* values only slightly greater than the 0.5 value which corresponds to a standard Brownian motion. *H* is shown to be greater in the western and lower latitudes. In contrast, temperature and PET show a higher degree of persistence in many locations, particularly in the western United States.

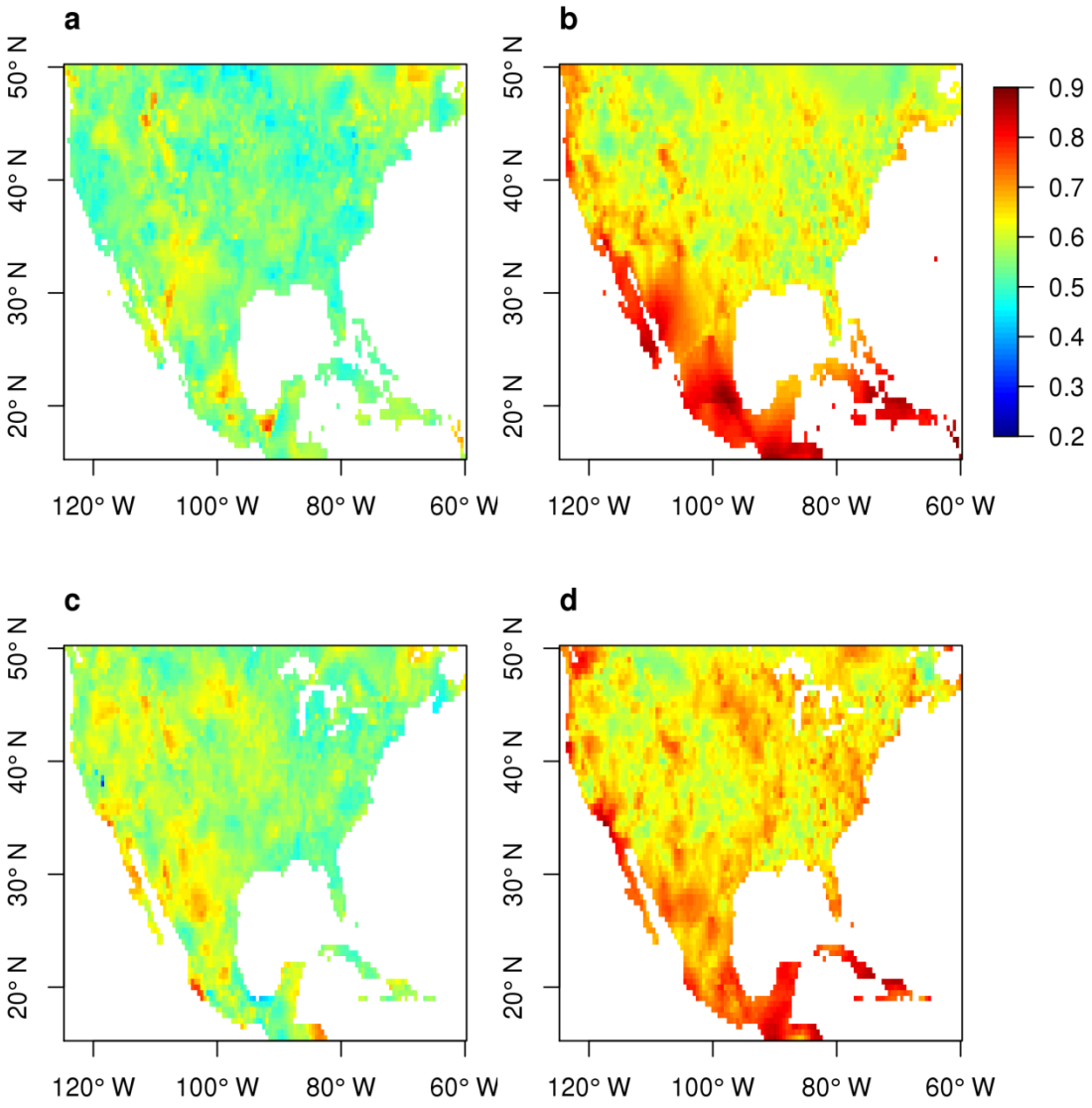

Figure 3.2: Hurst exponent estimated by scaled variance ratio method: (a) Precipitation, (b) Temperature, (c) SPEI, (d) PET.

However, what do these patterns of persistence "mean?" Intuition tells us that the higher the "persistence," the less erratic a time series is. The PET time series is taken as an example to examine this. This is borne out in these grid points, where higher *H* is generally characterized by higher absolute areas under the curve and fewer crossings of the zero-line (Fig. 3.3). So a higher persistence or *H* means that the cumulative quantity tends to stray away from the expected value for longer periods of time and its deficit/excess is greater than would be the case for a lower *H*. These results illustrate intuitively how *H* is a useful way to examine the behavior of cumulative departures. While it can be useful to look at the persistence of the quantities themselves, using *H* to analyze cumulative departures from expected values provides an insight into how far and how often a system strays from its expected behavior. This approach can therefore lend itself to practical applications in terms of resource management.

While Velasquez-Valle et al. [2013] found that *H* was dependent on annual precipitation, we find poor correlations between *H* and annual totals for all our quantities. However, this difference may be explained by the fact that, as shown above, *H* is dependent on the area under the curve, which in the case of Velasquez Valle et al. [2013] would have been related to annual precipitation. This difference further highlights the value of estimating persistence on departures from expected values rather than the absolute value of a time series if the goal is to estimate persistence of anomalously high or low values. We also find that *H* is not dependent on the number of significant coefficients (Fig. A3.3), although the lowest number of coefficients do tend to have lower *H* values. Thus, it is possible to have a variety of persistence structures with the same order of autoregression.

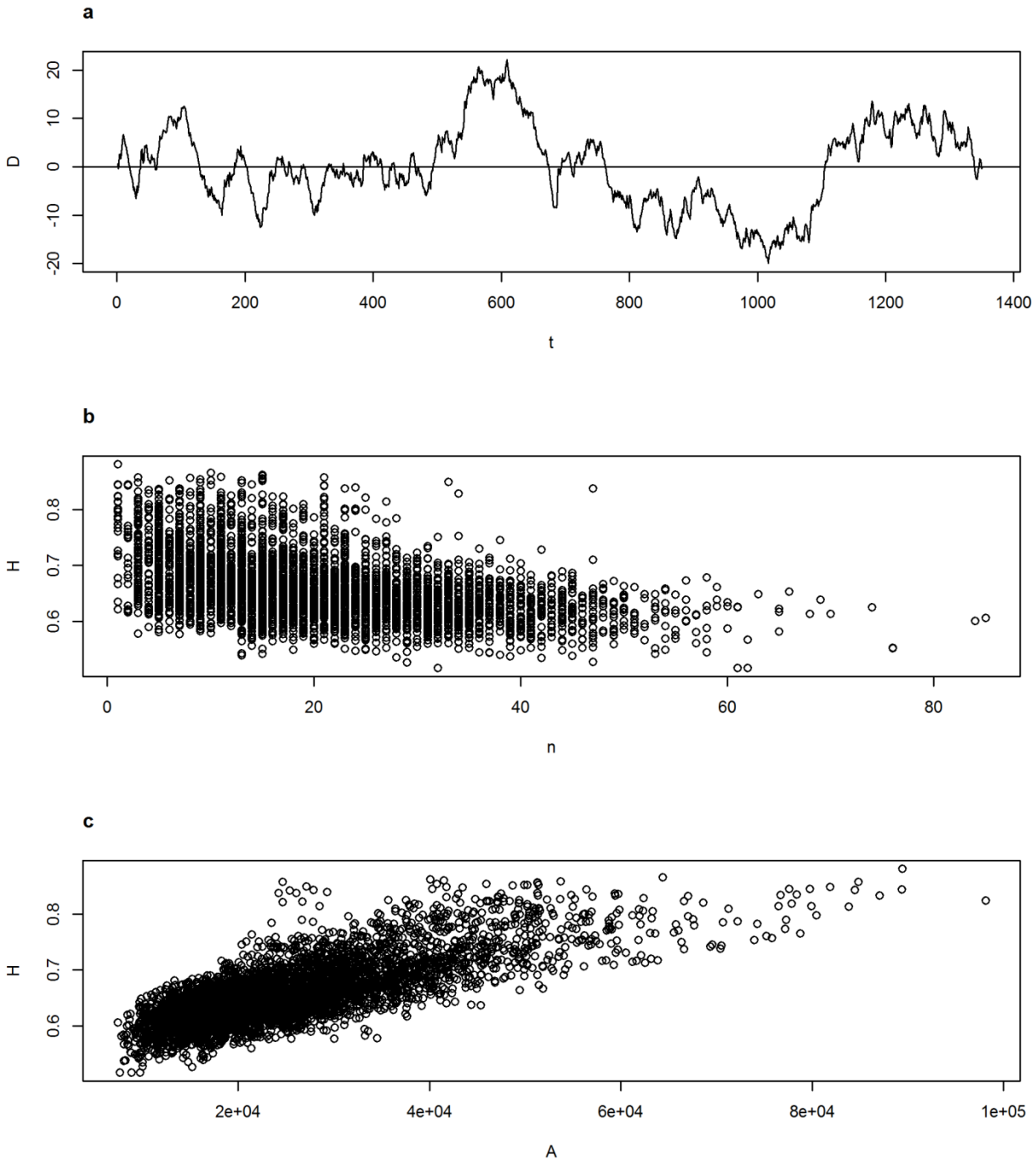

Figure 3.3: (a) A sample time series of cumulative departures D versus t, the number of months since the start of the record (the horizontal line is at D = 0); (b) Hurst exponent of PET against n, the number of times D crosses the zero line; (c) Hurst exponent of PET against A, the absolute area under the curve, i.e. the total area bounded by D.

To our knowledge, no other studies have compared the spatial patterns in *H* between the different time series considered here. Few studies have even explored the spatial variation in *H* in a single time series. Miranda et al. [2004] and Velasquez Valle et al. [2013] found *H* of precipitation was related to latitude and longitude in northeast Brazil and central Mexico, indicating that *H* varies with location. That *H* should vary by location appeals to intuition since the processes that cause persistence in a time series are likely to vary spatially. Brunsell [2010] showed that entropy of daily precipitation decreases from west to east in the United States. This is somewhat similar to what we find in our study, although the extent of the region with a significantly high persistence is much smaller in our case.

It is as yet unclear as to what physical processes cause these spatial patterns, though a visual comparison of Fig. 3.2 with Fig. 4 in Dirmeyer and Brubaker [2007] suggests that precipitation recycling ratios may account at least partly for the spatial pattern of *H* in precipitation. Additional support for this hypothesis may come from the observation that the areas with higher degrees of recycling tend to show higher values of *H* for both precipitation and temperature. PET *H* is well correlated with temperature *H* (Fig. 3.4) although, in general, it tends to be higher than temperature *H* at lower values and lower than it at higher values. These differences could be explained in part by taking into account the persistence of cloud cover and vapor pressure (not shown).

While the SPEI is dependent on both PET and P, it can be seen that its persistence is dependent much more on that of precipitation than PET (Fig. 3.4). Like, P, it tends also to have a lower persistence than PET. A comparison of the overlap of significant lags may make the relationships between time series clearer. The top half of Fig. 3.5 shows the proportion of

significant PET restricted autoregression lags that overlap with temperature and precipitation. These clearly show that PET autoregression lags shows a moderate to high degree of overlap with temperature autoregression lags: at least half of PET lags overlap with temperature lags in 40% of grid cells. In contrast, there is little matching between lags of PET versus P, with at least

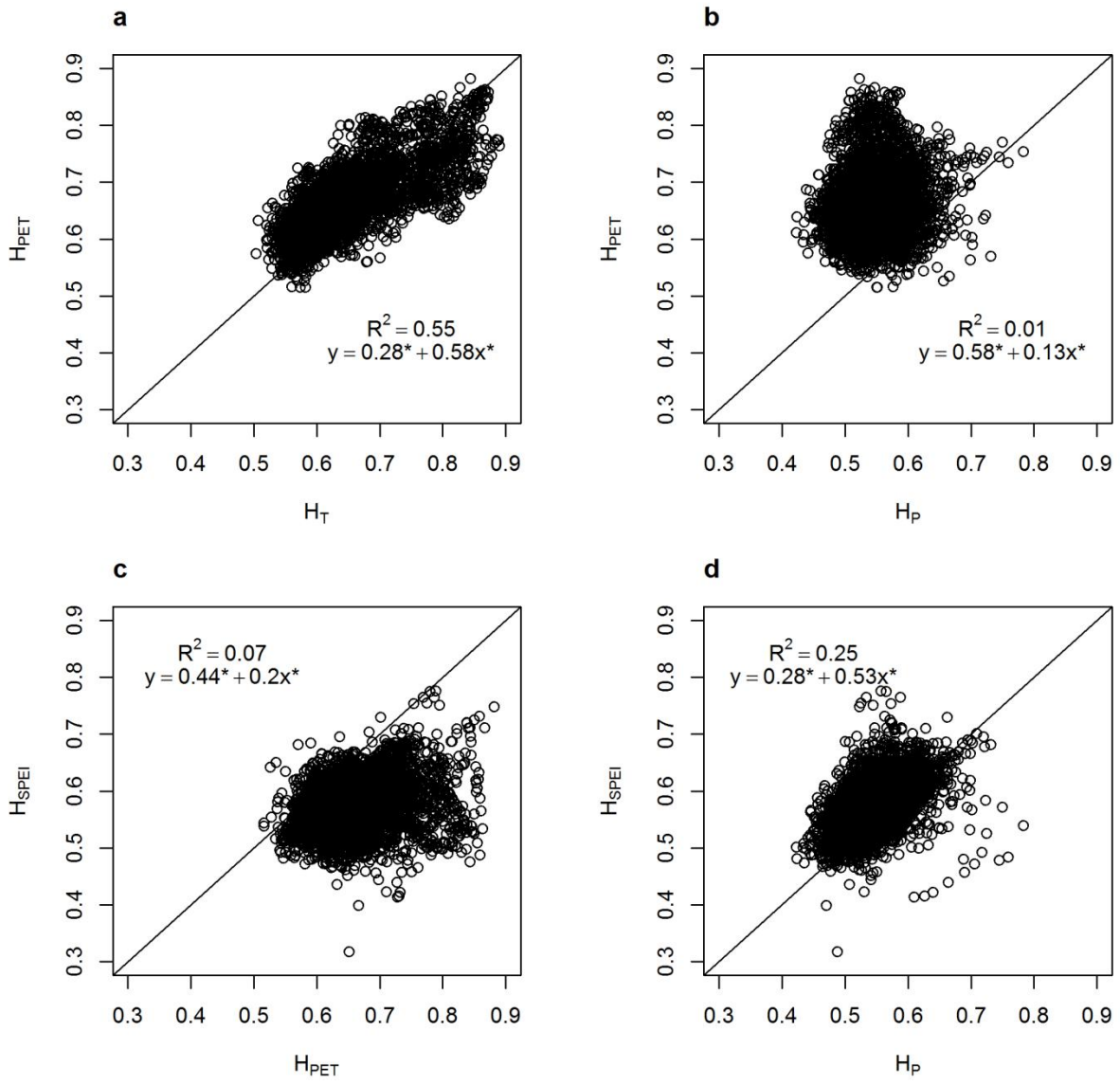

Figure 3.4: Hurst exponents plotted against each other: (a)PET *H* against temperature *H;* (b) PET *H* against precipitation *H*; (c) SPEI *H* against PET *H*; (d) SPEI *H* against precipitation *H*. Lines shown are of intercept 0 and slope 1. Asterisks in equations indicate coefficients are significant ($p<0.05$).

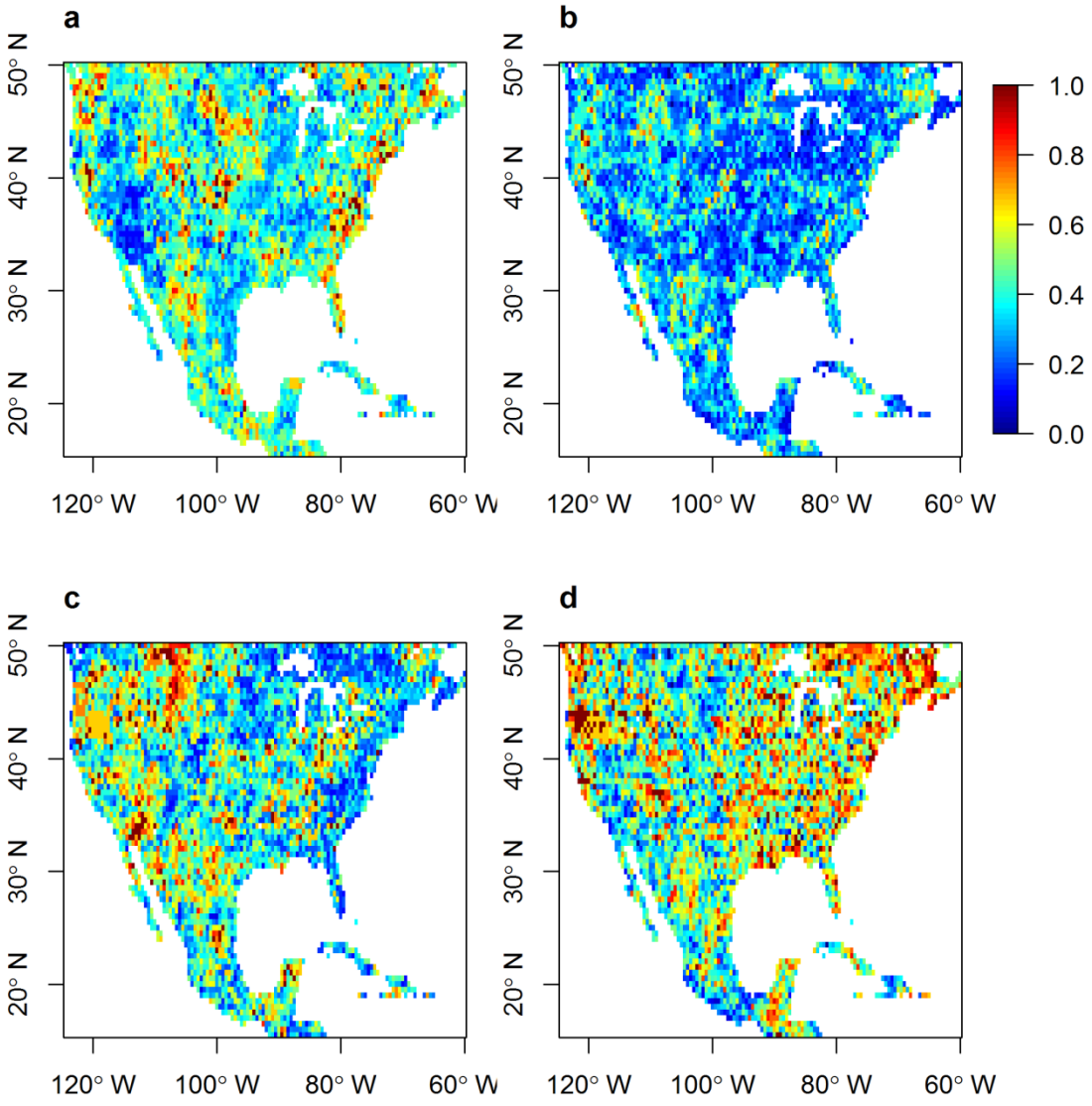

Figure 3.5: Proportion of matching coefficients: (a) number of matching coefficients between PET and Temperature, divided by number of coefficients of PET; (b) number of matching coefficients between PET and Precipitation, divided by number of coefficients of PET; (c) number of matching coefficients between SPEI and PET, divided by number of coefficients of SPEI; (d) number of matching coefficients between SPEI and P, divided by number of coefficients of SPEI.

half of PET lags overlapping with precipitation lags in only 14% of grid cells. For SPEI (bottom half of Fig. 3.5), there is a better degree of overlap with PET in the west than in the east. SPEI

autoregression lags overlap with precipitation autoregression lags mostly in the east but also in parts of the west. Overall, SPEI seems to match more with precipitation than with PET as the visual comparison of *H* for the various time series in Figs. 3.2 and A3.2 indicates. At least half of SPEI lags overlap with precipitation lags in 59% of the grid cells, whereas at least half of SPEI lags overlap with PET lags in only 42% of grid cells (Fig. 3.5). Note however that just because the significant lags are the same for two time series, their *H*s need not be the same or vice versa. This can be seen in the form of Eq. 6. Rather, we suggest that given similar *H* in two time series at a location, a comparison of their significant lags in the autoregression may provide insights on the time scales of the mechanisms that affect each.

Previous studies have indicated that trends in both precipitation and temperature (through potential evapotranspiration) have contributed to trends in drought. However, they have also found regional differences in the impact of each of these quantities: e.g. Briffa et al [2009] found in a study of very long European records that the influence of increasing temperature trends on the self-calibrating Palmer Drought Severity Index (scPDSI) is particularly strong in central Europe while Dai [2012] found that trends in precipitation and the scPDSI are similar globally, including in North America. The relative influence of evapotranspiration and PET on drought has been the subject of some discussion [*Dai*, 2011; *Vicente-Serrano et al.*, 2011]. Here we use a PET-based index and find that even in it, the correlation of PET persistence and drought persistence may be quite high in some places but quite low in others (Fig. 3.5). This is not counter-intuitive since the relative importance of precipitation and PET can be expected to vary based on location. The analysis presented here provides one way to compare the persistence of different time series.

Conclusions

We show here that cumulative departures of precipitation, temperature, PET and SPEI can be modeled using a simple autoregressive approach that is consistent with their persistence characteristics. We also show that this implies that the departures are stationary in time, i.e. there is no evidence for an increase in variability in these time series at the monthly scale. Persistence, as estimated by the Hurst exponent, is shown to be related to simple measures of the cumulative departure time series, such as the area under the curve and the number of times the curve crosses the zero line. The use of the autoregressive approach allows the comparison of the relative influence of different time series, e.g. of precipitation and PET on the SPEI.

References

Allen, R. G., L. S. Pereira, D. Raes, and M. Smith (1988), *Crop evapotranspiration - Guidelines for computing crop water requirements - FAO Irrigation and drainage paper 56*, Food and Agriculture Organization of the United Nations.

Alvarez-Ramirez, J., J. C. Echeverria, and E. Rodriguez (2011), Is the North Atlantic Oscillation modulated by solar and lunar cycles? Some evidences from Hurst autocorrelation analysis, *Adv. Space Res.*, *47*(4), 748–756, doi:10.1016/j.asr.2010.09.030.

Beguería, S., S. M. Vicente-Serrano, and M. Angulo-Martínez (2010), A Multiscalar Global Drought Dataset: The SPEIbase: A New Gridded Product for the Analysis of Drought Variability and Impacts, *Bull. Am. Meteorol. Soc.*, *91*(10), 1351–1356, doi:10.1175/2010BAMS2988.1.

Bierkens, M. F. P., and B. J. J. M. van den Hurk (2007), Groundwater convergence as a possible mechanism for multi-year persistence in rainfall, *Geophys. Res. Lett.*, *34*(2), doi:10.1029/2006GL028396.

Briffa, K. R., G. van der Schrier, and P. D. Jones (2009), Wet and dry summers in Europe since 1750: evidence of increasing drought, *Int. J. Climatol.*, *29*(13), 1894–1905, doi:10.1002/joc.1836.

Brunsell, N. A. (2010), A multiscale information theory approach to assess spatial–temporal variability of daily precipitation, *J. Hydrol.*, *385*(1-4), 165–172, doi:10.1016/j.jhydrol.2010.02.016.

Cannon, M. J., D. B. Percival, D. C. Caccia, G. M. Raymond, and J. B. Bassingthwaighte (1997), Evaluating scaled windowed variance methods for estimating the Hurst coefficient of time series, *Phys. Stat. Mech. Its Appl.*, *241*(3-4), 606–626, doi:10.1016/S0378-4371(97)00252-5.

Computational and Information Systems Laboratory (2012), *Yellowstone: IBM iDataPlex System (University Community Computing)*, National Center for Atmospheric Research, Boulder, Colorado.

CRU (n.d.), Viewing CRU TS3.10: Climatic Research Unit (CRU) Time-Series (TS) Version 3.10 of High Resolution Gridded Data of Month-by-month Variation in Climate (Jan. 1901 - Dec. 2009), Available from: http://badc.nerc.ac.uk/view/badc.nerc.ac.uk__ATOM__ACTIVITY_fe67d66a-5b02-11e0-88c9-00e081470265 (Accessed 9 June 2014)

Dai, A. (2011), Characteristics and trends in various forms of the Palmer Drought Severity Index during 1900–2008, *J. Geophys. Res.*, *116*(D12), doi:10.1029/2010JD015541.

Dai, A. (2012), Increasing drought under global warming in observations and models, *Nat. Clim. Change*, *3*(1), 52–58, doi:10.1038/nclimate1633.

Dirmeyer, P. A., and K. L. Brubaker (2007), Characterization of the Global Hydrologic Cycle from a Back-Trajectory Analysis of Atmospheric Water Vapor, *J. Hydrometeorol.*, *8*(1), 20–37, doi:10.1175/JHM557.1.

Hurst, H. (1950), Long-term storage capacity of reservoirs, *Proc Amer Soc Civ. Eng*, *76*.

IPCC (2013), *Climate Change 2013: The Physical Science Basis.*

Kantelhardt, J. W., E. Koscielny-Bunde, D. Rybski, P. Braun, A. Bunde, and S. Havlin (2006), Long-term persistence and multifractality of precipitation and river runoff records, *J. Geophys. Res.*, *111*(D1), doi:10.1029/2005JD005881.

Karl, T. R., R. W. Knight, and N. Plummer (1995), Trends in high-frequency climate variability in the twentieth century, *Nature*, *377*(6546), 217–220, doi:10.1038/377217a0.

Klemeš, V. (1974), The Hurst Phenomenon: A puzzle?, *Water Resour. Res.*, *10*(4), 675–688, doi:10.1029/WR010i004p00675.

Mandelbrot, B. B. (1977), *Fractals: form, chance, and dimension*, W. H. Freeman, San Francisco.

Matsoukas, C., S. Islam, and I. Rodriguez-Iturbe (2000), Detrended fluctuation analysis of rainfall and streamflow time series, *J. Geophys. Res.*, *105*(D23), 29165, doi:10.1029/2000JD900419.

McKenney, D. W., J. H. Pedlar, P. Papadopol, and M. F. Hutchinson (2006), The development of 1901–2000 historical monthly climate models for Canada and the United States, *Agric. For. Meteorol.*, *138*(1-4), 69–81, doi:10.1016/j.agrformet.2006.03.012.

Miranda, J. G. V., R. F. S. Andrade, A. B. da Silva, C. S. Ferreira, A. P. Gonzalez, and J. L. Carrera L�pez (2004), Temporal and spatial persistence in rainfall records from Northeast Brazil and Galicia (Spain), *Theor. Appl. Climatol.*, *77*(1-2), 113–121, doi:10.1007/s00704-003-0013-8.

Peng, C.-K., S. Buldyrev, S. Havlin, M. Simons, H. Stanley, and A. Goldberger (1994), Mosaic organization of DNA nucleotides, *Phys. Rev. E*, *49*(2), 1685–1689, doi:10.1103/PhysRevE.49.1685.

R Core Team (2013), *R: A Language and Environment for Statistical Computing*, R Foundation for Statistical Computing, Vienna, Austria.

Sun, F., M. L. Roderick, and G. D. Farquhar (2012), Changes in the variability of global land precipitation, *Geophys. Res. Lett.*, *39*(19), n/a–n/a, doi:10.1029/2012GL053369.

Triacca, U., A. Pasini, and A. Attanasio (2014), Measuring persistence in time series of temperature anomalies, *Theor. Appl. Climatol.*, doi:10.1007/s00704-013-1076-9.

Tsonis, A. A. (1996), Widespread increases in low-frequency variability of precipitation over the past century, *Nature*, *382*(6593), 700–702, doi:10.1038/382700a0.

Turvey, C. G. (2007), A note on scaled variance ratio estimation of the Hurst exponent with application to agricultural commodity prices, *Phys. Stat. Mech. Its Appl.*, *377*(1), 155–165, doi:10.1016/j.physa.2006.11.022.

Valle, M. A. V., G. M. García, I. S. Cohen, L. Klaudia Oleschko, J. A. Ruiz Corral, and G. Korvin (2013), Spatial Variability of the Hurst Exponent for the Daily Scale Rainfall Series in the State of Zacatecas, Mexico, *J. Appl. Meteorol. Climatol.*, *52*(12), 2771–2780, doi:10.1175/JAMC-D-13-0136.1.

Vicente-Serrano, S. M., S. Beguería, and J. I. López-Moreno (2010a), A Multiscalar Drought Index Sensitive to Global Warming: The Standardized Precipitation Evapotranspiration Index, *J. Clim.*, *23*(7), 1696–1718, doi:10.1175/2009JCLI2909.1.

Vicente-Serrano, S. M., S. Beguería, J. I. López-Moreno, M. Angulo, and A. El Kenawy (2010b), A New Global 0.5° Gridded Dataset (1901–2006) of a Multiscalar Drought Index: Comparison with Current Drought Index Datasets Based on the Palmer Drought Severity Index, *J. Hydrometeorol.*, *11*(4), 1033–1043, doi:10.1175/2010JHM1224.1.

Vicente-Serrano, S. M., S. Beguería, and J. I. López-Moreno (2011), Comment on "Characteristics and trends in various forms of the Palmer Drought Severity Index (PDSI) during 1900–2008" by Aiguo Dai, *J. Geophys. Res.*, *116*(D19), doi:10.1029/2011JD016410.

Wongsasutthikul, P., and C. G. Turvey (2011), An Autoregressive Approach to Modeling Fractional Brownian Motion (Unpublished).

CONCLUSIONS

The results presented here suggest several further questions for exploration. Those that are planned for the immediate future are briefly described. The first chapter showed that the start of the rainy season in India has been shifting earlier. Since this time of the year is extremely important to agriculture in India, most of which is exclusively or mostly rainfed, the effect of the changing start dates on agriculture will be examined. This will be done by regression of the rainy season start dates at each pixel against the maximum growing season Normalized Difference Vegetation Index (NDVI) data for that pixel. Regressions will also be conducted at a district level against crop yield data obtained from the International Crops Research Institute for the Semi-Arid Tropics (ICRISAT).

Secondly, the simple water balance method used in the second chapter will be extended to the other sub-basins of the Mississippi, namely the Upper-Mississippi, the Ohio-Tennessee and the Lower Mississippi. The sub-basins have very different climatic and ecological characteristics, and comparing trends in storage and evapotranspiration amongst them and the basin as a whole is likely to produce new insights on the system. Finally, in the same study, the one parameter (α) in the model was assumed to be constant for a given basin over the entire time period. The temporal and spatial variability of α will be examined by using Moderate Resolution Imaging Spectrometer (MODIS) based evapotranspiration and potential evapotranspiration products in combination with Gravity Recovery and Climate Experiment (GRACE) based storage anomaly data to specify the other quantities in Eq. 2 of that chapter. It is expected that α will not vary significantly in time but will be significantly dependent on the climatic and ecological

characteristics of the river basin. Knowing the nature of variation of α will lead to further insights on the physical meaning of this parameter.

APPENDIX 1

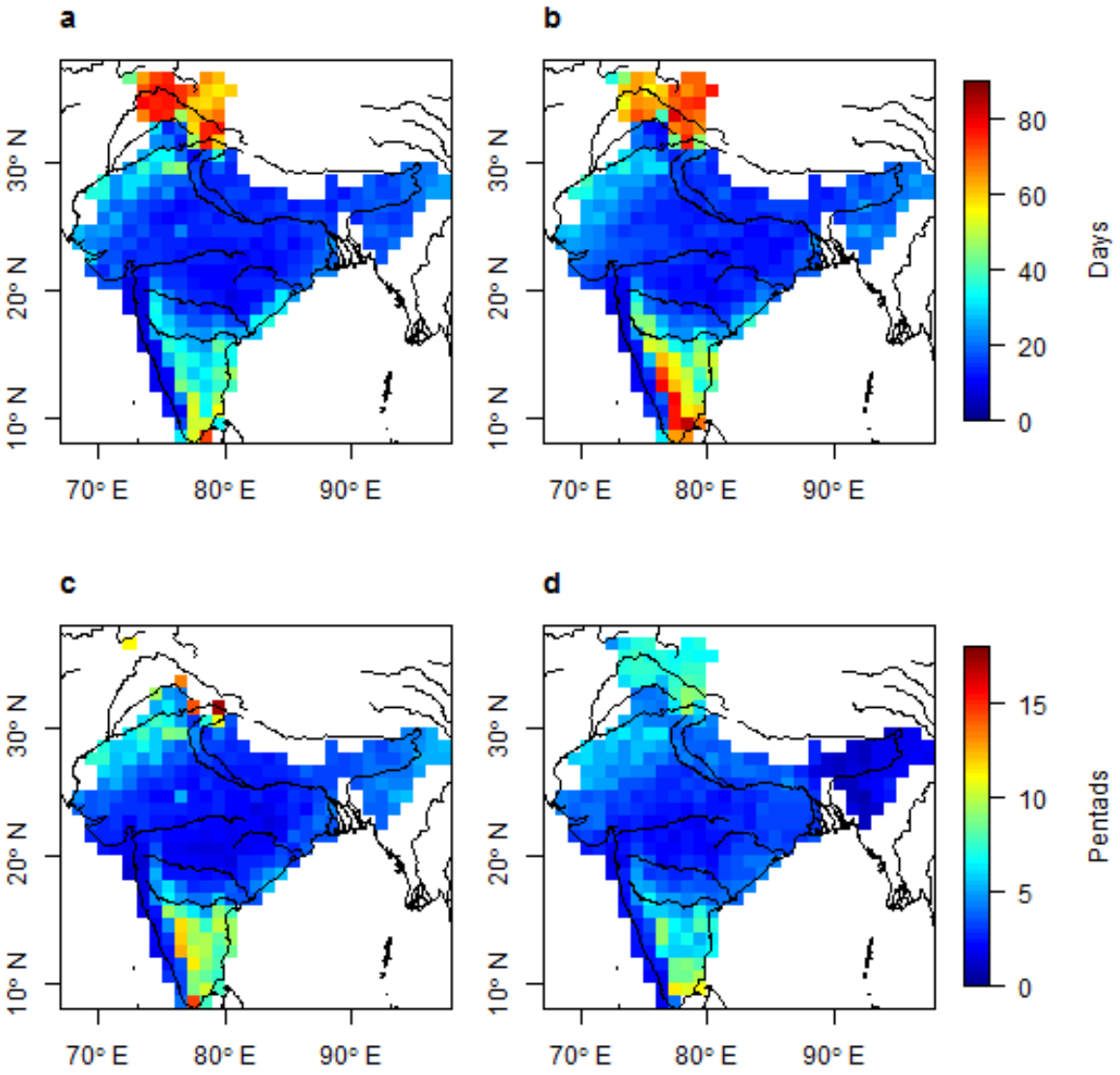

Figure A1.1: Standard deviation of the start of the rainy season for the period 1951-2007 determined by the (a) SS, (b) PL, (c) CD and (d) WL methods. In the CD method (c), the variability in the region above 30° N is not displayed as it is above the scale of the legend, which was chosen to illustrate the differences between regions and methods. Only grid cells with standard deviation less than or equal to 30 days for SS, PL and CD methods were selected for the rest of the analysis.

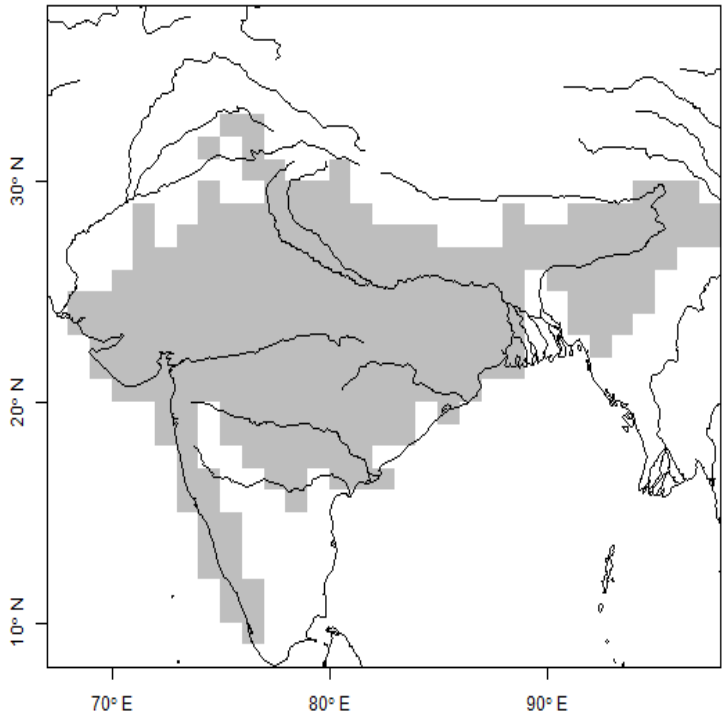

Figure A2.2: The study area, indicated by gray grid cells.

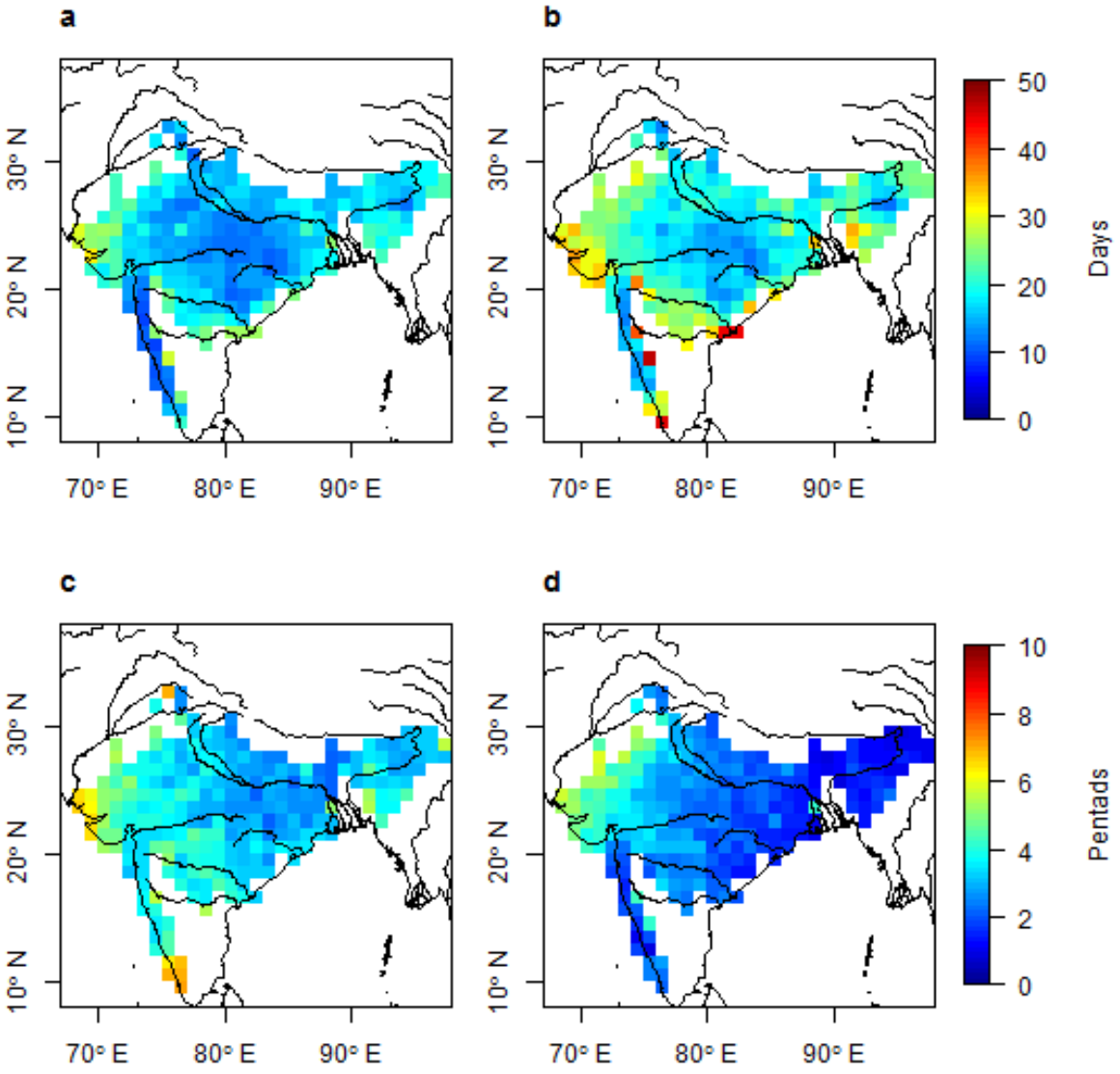

Figure A1.3: Standard deviation of the *end* of the rainy season for the period 1951-2007 determined by the (a) SS, (b) PL, (c) CD and (d) WL methods. Note different scale than used for Figure A1.

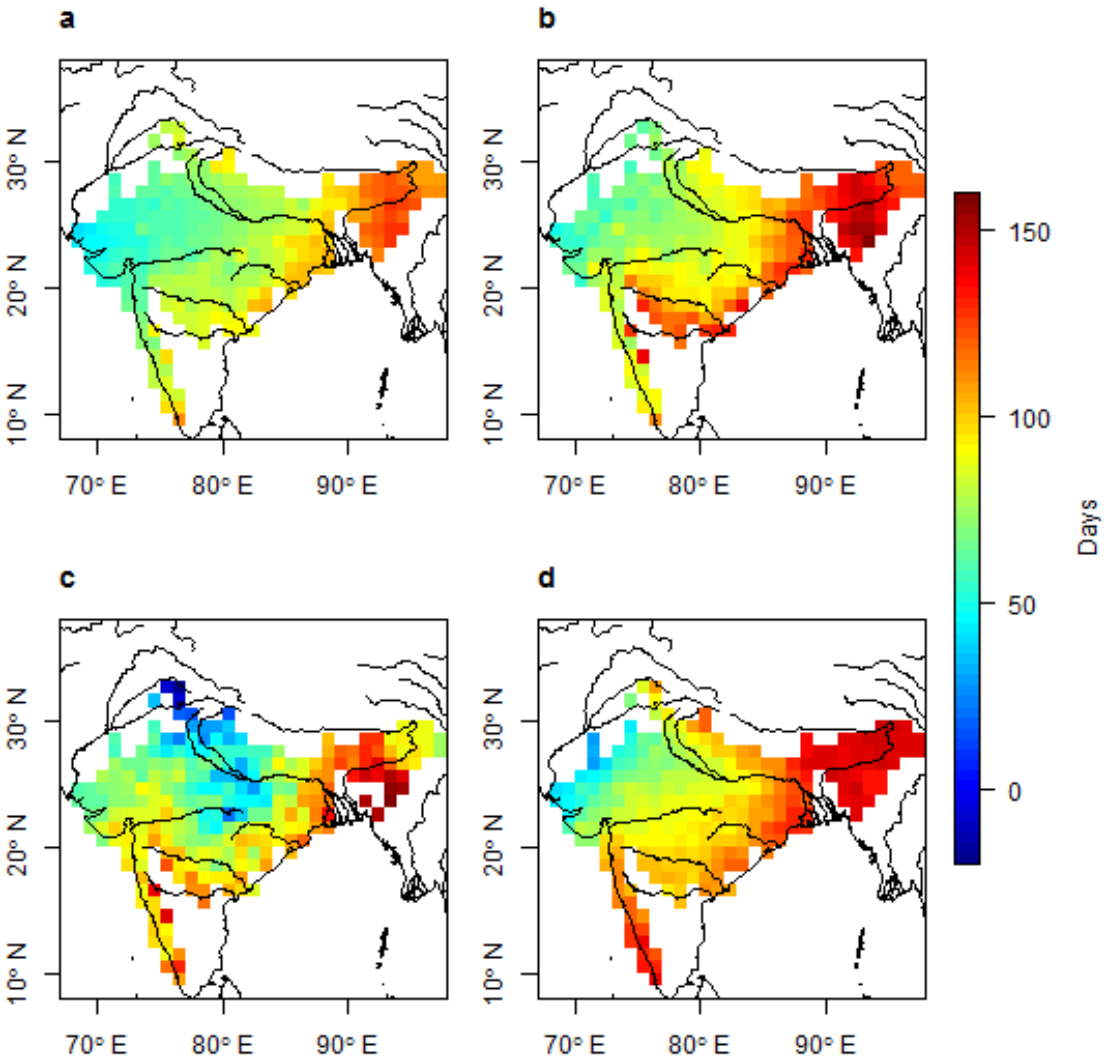

Figure A1.4: *Length* of the rainy season for the period 1951-2007 determined by the (a) SS, (b) PL, (c) CD and (d) WL methods.

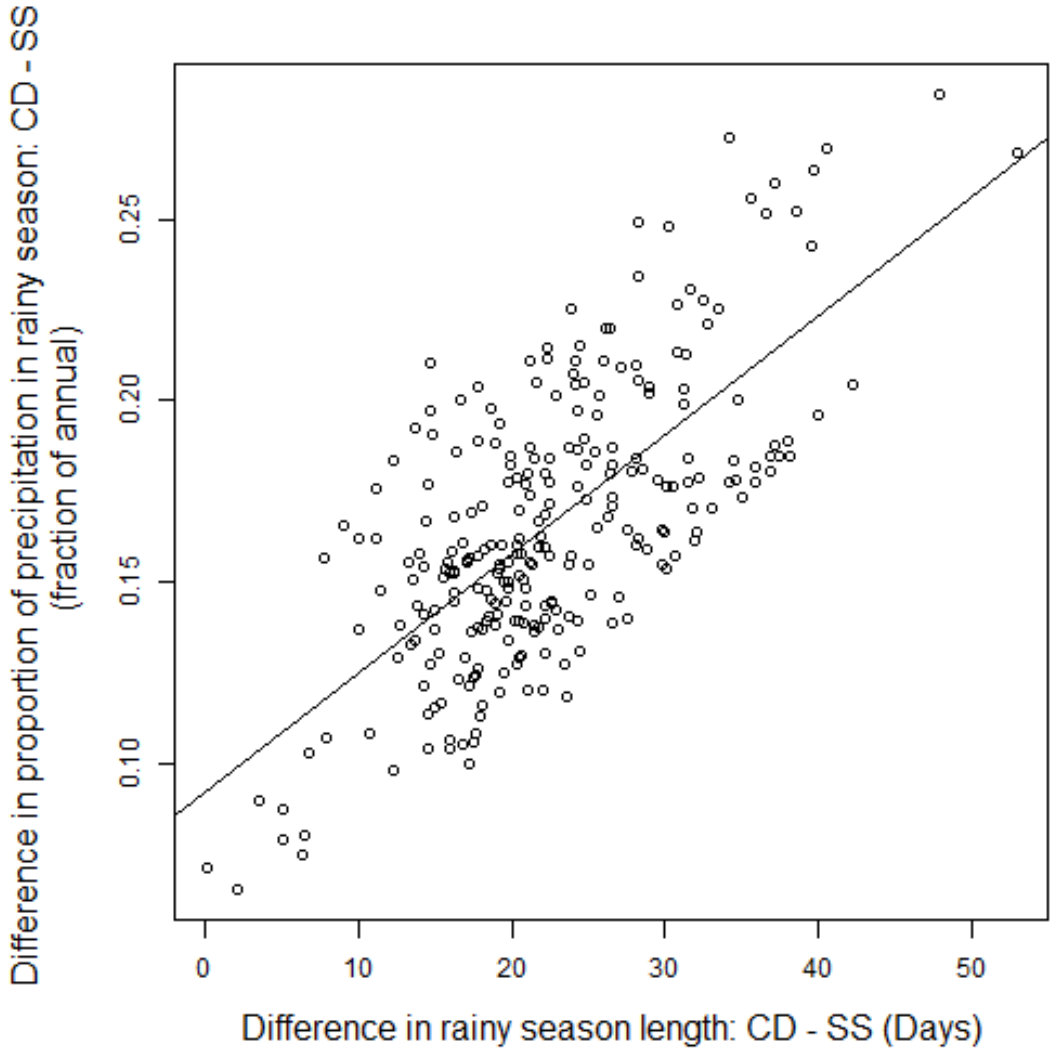

Figure A1.5: Fraction of excess precipitation in the CD rainy season (compared to the SS rainy season) plotted against the excess days in the CD rainy season (compared to the SS rainy season).

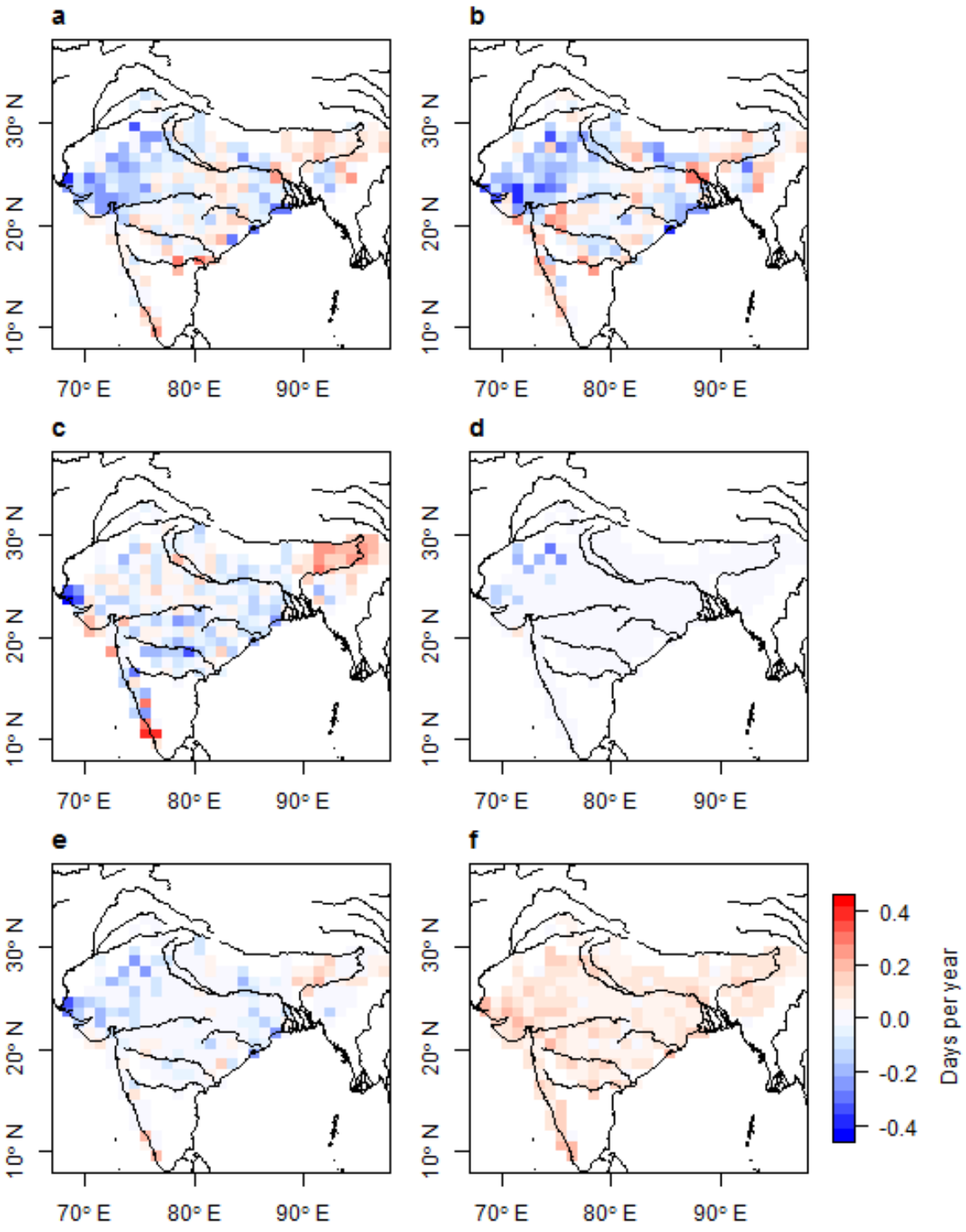

Figure A1.6: Trend in *end* of the rainy season for the period 1951-2007 determined by the (a) SS, (b) PL, (c) CD and (d) WL methods; (e) the median trend and (f) the standard deviation of the trends. Non-zero median trends are shown only if three or more methods agreed on the direction of the trend.

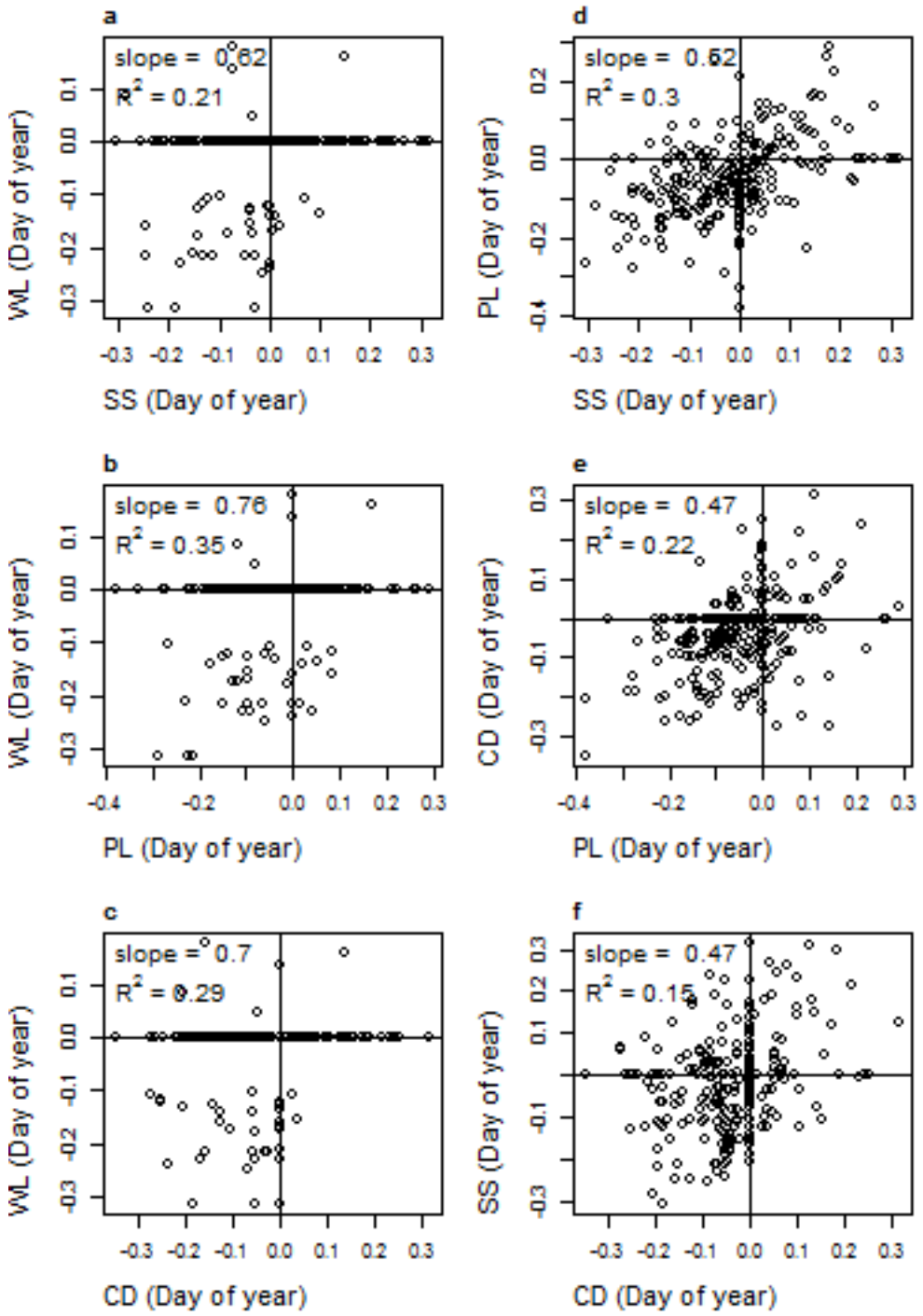

Figure A1.7: Trends (1951-2007) in the start date of the rainy season calculated by the various methods plotted against each other. The number of points in the upper right and bottom left

(upper left and bottom right) quadrants is: (a) 24 (9), (b) 24 (10), (c) 23 (5), (d) 149 (64), (e) 126 (42), and (f) 111 (56).

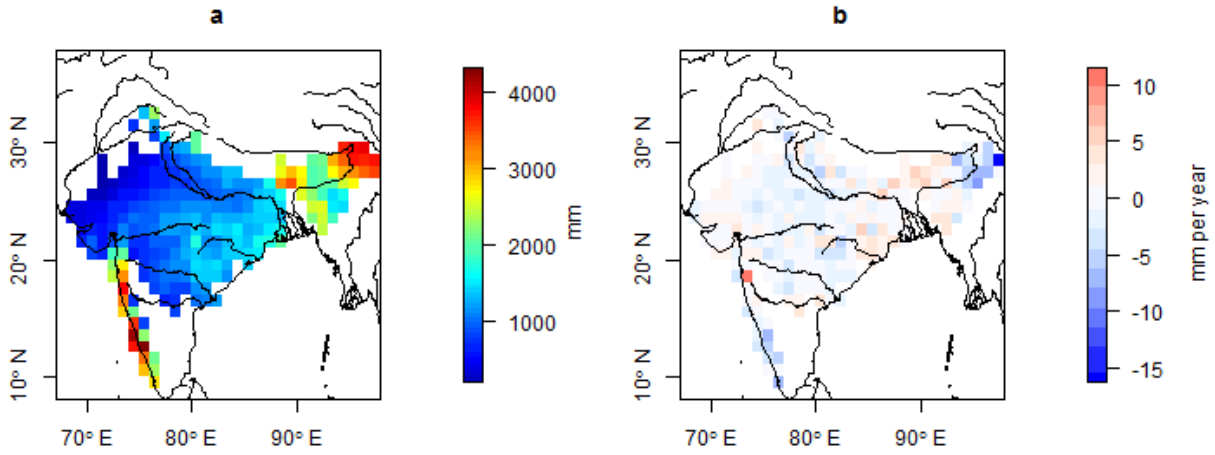

Figure A1.8: Trend (a) in and mean amount (b) of annual total precipitation for the period 1951-2007.

APPENDIX 2

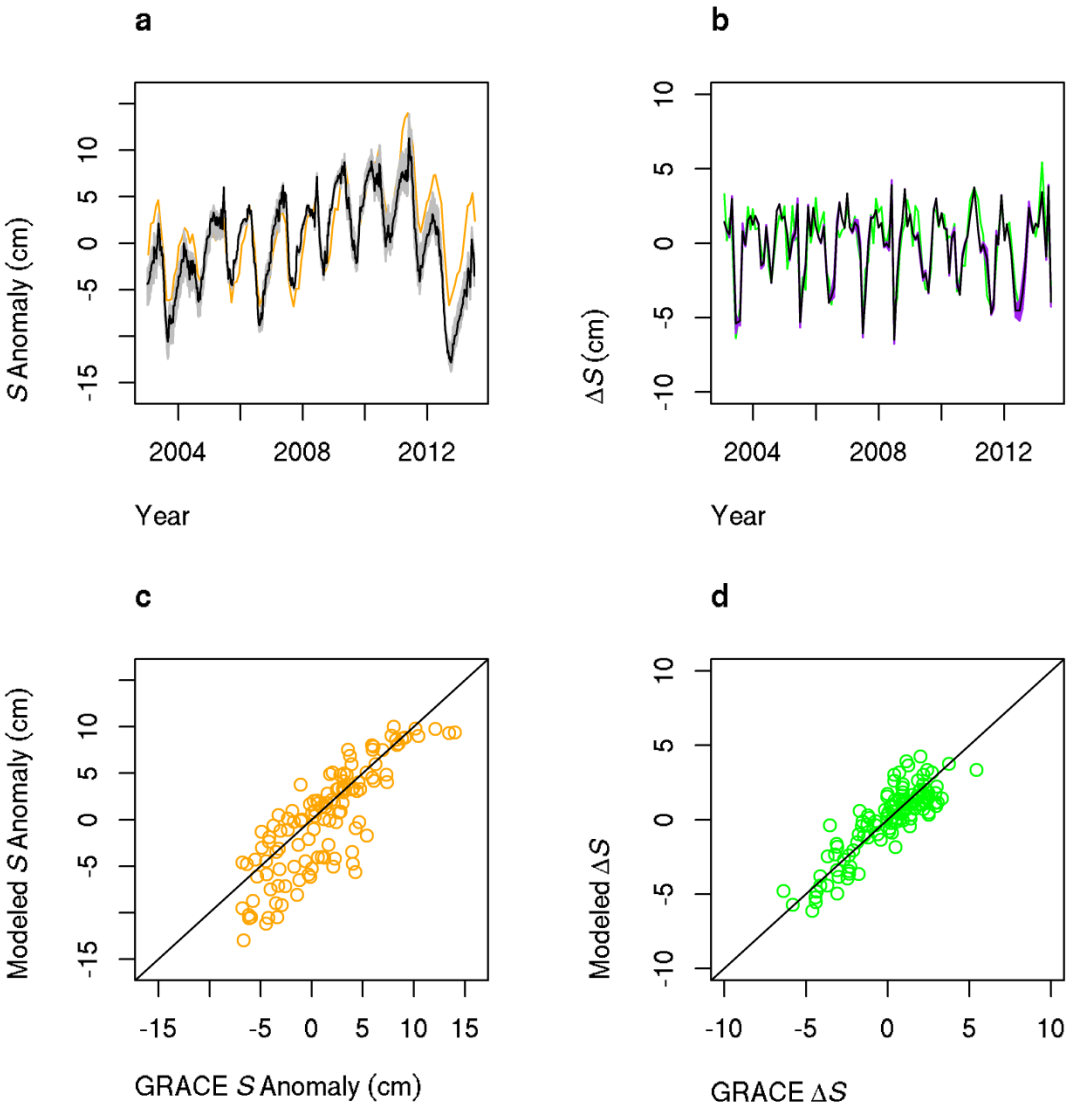

Figure A2.1: Modeled and GRACE data found by minimizing $SSR_{\Delta S}$: (a) S anomalies plotted as a time series; black lines are GRACE data. orange lines are the best (lowest *SSR*) modeled data, and gray lines are other modeled data within 5% of the lowest *SSR*. (b) ΔS plotted as a time series; black lines are GRACE data. green lines are the best (lowest *SSR*) modeled data, and purple lines (barely visible) are other modeled data within 5% of the lowest *SSR*. (c) S anomalies, modeled (best (lowest *SSR*) modeled data) v. observed, and (d) ΔS, modeled (best (lowest *SSR*) modeled data) v. observed. In (c) and (d), lines shown to facilitate comparison have intercept = 0 and slope = 1.

APPENDIX 3

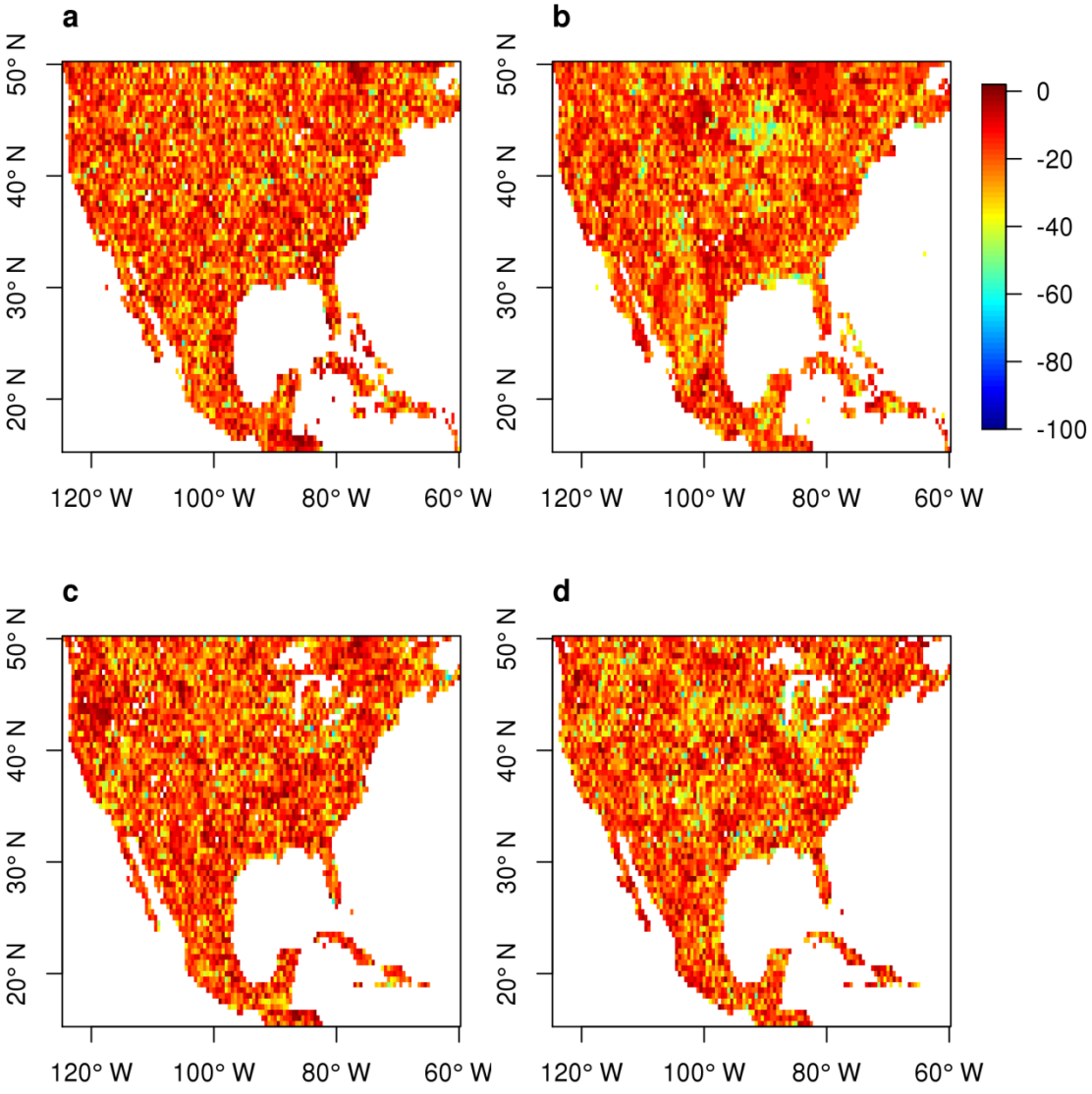

Figure A3.1: BIC of unrestricted model subtracted from BIC of restricted autoregressive model with coefficient sums forced to equal one: (a) Precipitation, (b) Temperature, (c) SPEI, (d) PET. The scale goes from -100 to +2. Models are considered statistically equivalent up to a difference of 2 points. In most locations, the BIC of the restricted model is much lower than that of the unrestricted model by more than two points, implying that the restricted model is better.

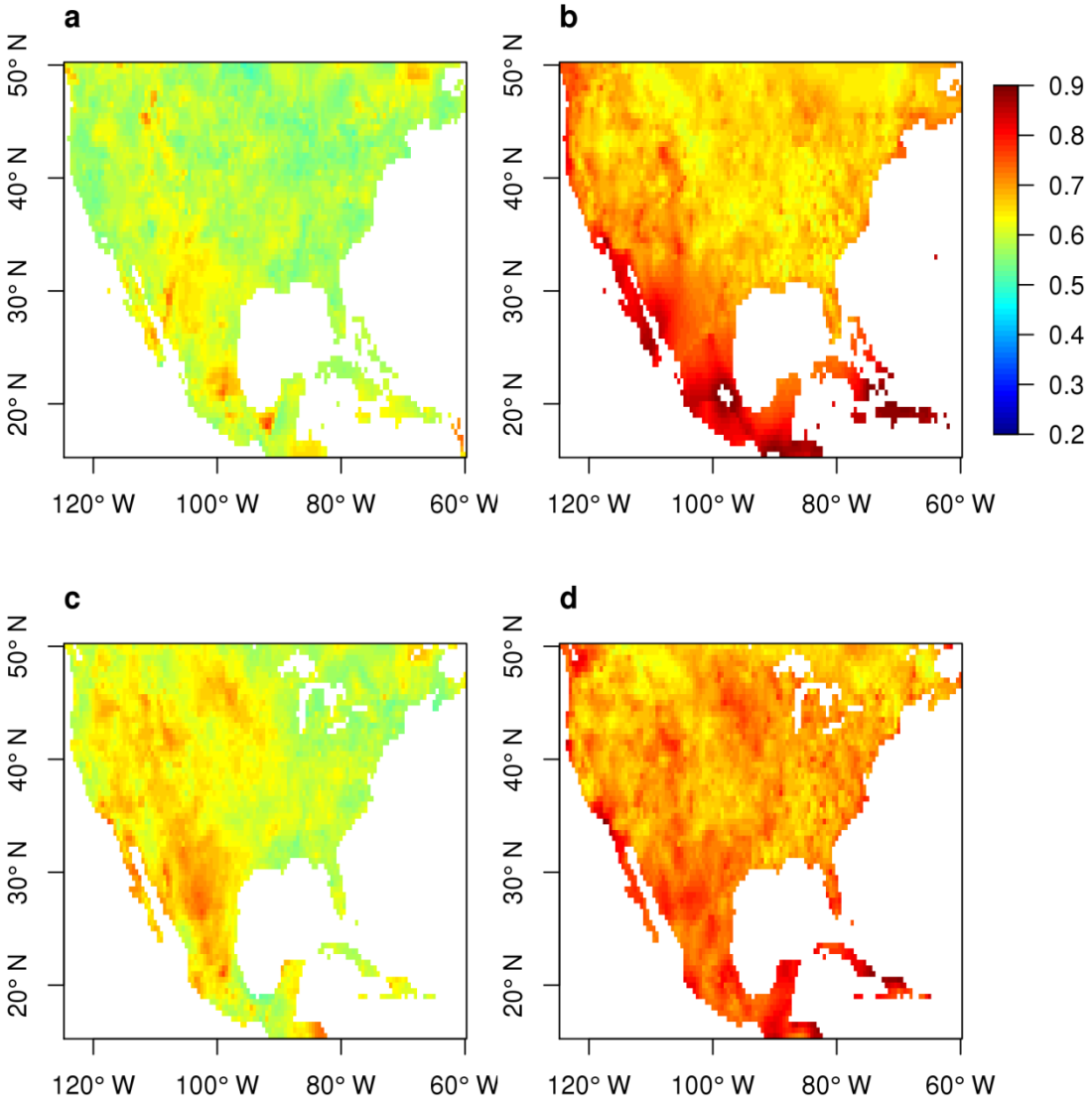

Figure A3.2: Hurst exponent estimated by detrended fluctuation analysis method: (a) Precipitation, (b) Temperature, (c) SPEI, (d) PET.

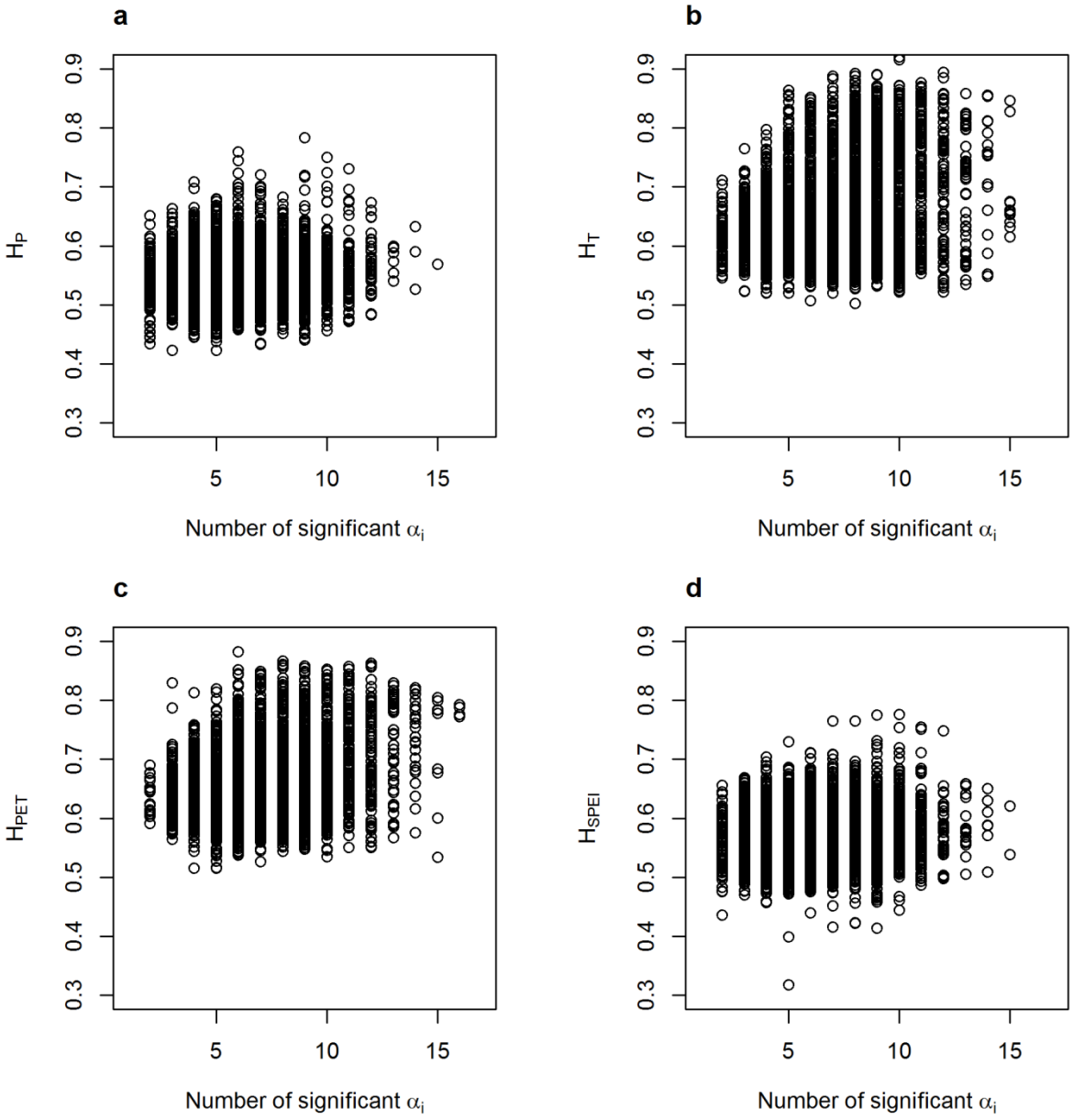

Figure A3.3: Hurst exponent against *number* of significant coefficients in the restricted autoregression: (a) Precipitation, (b) Temperature, (c) SPEI, (d) PET.